FABRICATION AND CHARACTERISATION OF SOLID-STATE PEROVSKITE SOLAR CELLS USING PLATINUM-BASED MULTIWALLS CARBON NANOTUBES AS COUNTER ELECTRODE.

BY

IBRAHIM, Olalonpe Sharifat

PhD/SNAS/2012/471

DEPARTMENT OF PHYSICS, SCHOOL OF PHYSICAL SCIENCES, FEDERAL UNIVERSITY OF TECNOLOGY MINNA.

INTRODUCTION

Energy consumption is one of the most important aspects in people's everyday life. It exists in different forms, from burning woods to obtain fire in prehistoric times to electricity productions in modern age.

Forms of energy

Mechanical, chemical, light, electrical

Challenges

Rapid growth in industrialisation worldwide, increased the demand in consumption of energy and as a result, the original sources of energy that the people used to harvest from, have shown signs of deficiency

Excessive emission of greenhouse gases, caused by burning fossil fuel, result in global warming threatening earth's ecosystem.

Waste disposal by people from nuclear power generation as a viable alternative to carbon based fuel.

Solution

Scientific focused on the design of technologies that utilises one of the primary renewable energy sources; water, biomass, wind, geothermal and solar irradiation for power generation.

Water

Biomass

Solution continues

Wind

Geothermal

Solar

Photovoltaic Technology

Photovoltaic (PV), also called solar cells, are electronic devices that convert sunlight directly into electricity.

Solar cell generations

- First generation: Crystalline Silicon Cells.
- Second generation: Thin-Film Solar Cells.
- Third-generation: New concept

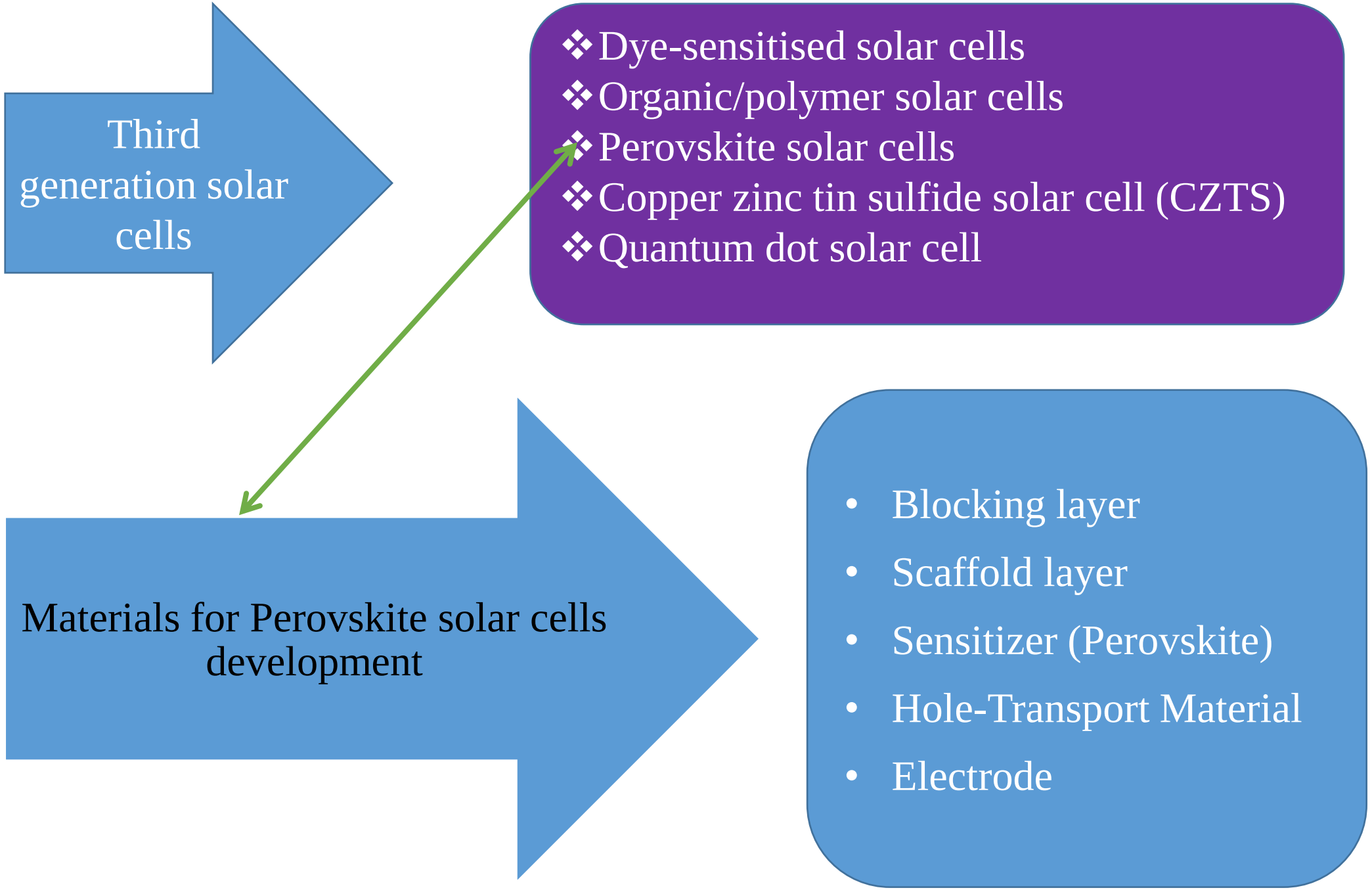
Third generation solar cells
❖Dye-sensitised solar cells
❖Organic/polymer solar cells
❖Perovskite solar cells
❖Copper zinc tin sulfide solar cell (CZTS)
❖Quantum dot solar cell
Materials for Perovskite solar cells development
• Blocking layer
• Scaffold layer
• Sensitizer (Perovskite)
• Hole-Transport Material
• Electrode

ELECTRODE MATERIALS FOR SOLAR CELLS DEVELOPMENT

are

- ❖ Carbon electrodes
- ❖ Metal oxide electrodes
- ❖ Polymer electrodes
- ❖ Nanocomposite electrodes

Carbon electrodes are

- carbon nanotubes (CNTs)
- Graphene oxide (GO)
- Fullerene

Types of Carbon nanotubes (CNTs)

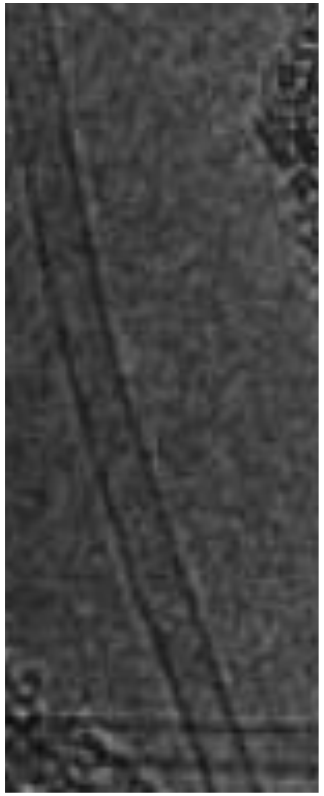

Single-walled

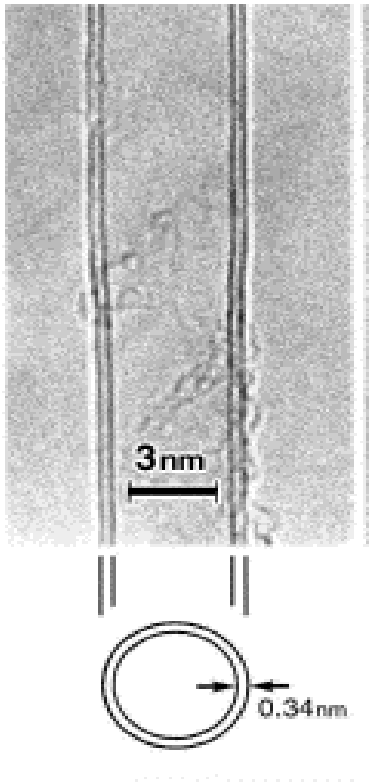

Double-walled

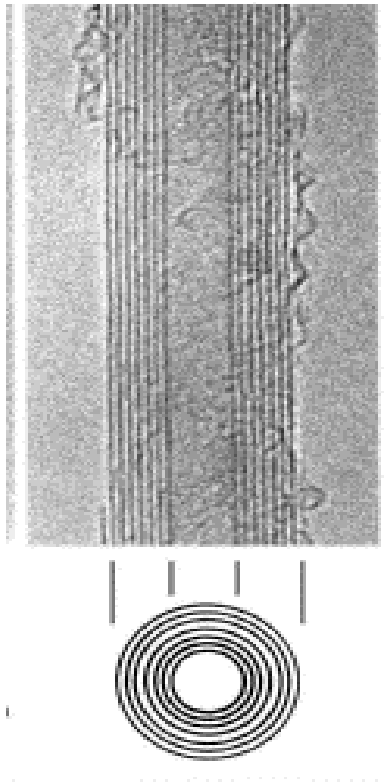

Multi-walled

Statement of the Problem

- High cost of fabrication of conventional silicon solar cells.
- They are heavily reliant on the weather.
- Use of high cost Platinum (Pt) as counter electrode.
- Their installation cost is higher than those of electrical systems.

The aim of this research work is to fabricate and characterized **dye sensitized solar cell** using platinum-based multiwall carbon nanotubes as counter electrode.

This aim was achieved through the following outline objectives;

- Produce Platinum multiwalled carbon nanotubes (Pt-MWCNTs)
- Characterized the Pt-MWCNTs produced
- Assembled the optimised component materials (FTO, TiO_2 compact layer, TiO_2 mesoporous layer, perovskite layer and Pt-MWCNT) together.
- Test for the performance evaluation of the solar cells

SIGNIFICANCE OF THE STUDY

- Commercial production of DSSCs by using affordable carbon materials as counter electrode.
- Providing alternative to the platinum-based counter electrode of DSSCs.
- To reduce the amount of pollution caused from using non-renewable energy resources, by producing a much safer renewable energy resources.

Scope of the study

This study focused on the synthesis of multiwall carbon nanotubes (MWCNTs) using catalytic vapour deposition (CVD) method. The as-synthesised MWCNTs were functionalised, characterised and then doped with platinum to produce Pt-MWCNTs catalyst as counter electrode. The DSSCs was then be fabricated by assembled the optimised component materials (FTO, TiO_2 compact layer, TiO_2 mesoporous layer, sensitizer, (dye) and Pt-MWCNT) together and the electrolyte was then injected into it. Finally the performance of the assembled solar cells was tested using solar simulator.

LITERATURE REVIEW

AUTHOR	WORKDONE	RESULTS/PCE	LIMITATIONS
Yasemin *et al.*, (2021)	Polypyrrole and multi-walled carbon nanotube (MWCNT) composite film was produced by electrochemical polymerization of pyrrole with MWCNT on ITO surface	2.60 %	The porous structure of PPy electrodeposed in MWCNT improved the roughness and specific surface area of the MWCNT and increased the electronic transmission capacity of PPy.
Wu & Wenjun, (2022)	A three component (MWCNTs, carbon black and graphite) carbon electrode material for DSSC devices combined with the advantages of high electron transfer kinetics of MWCNTs, plentiful catalytic sites in crystal edges of carbon black and superior electrical conductivity and catalytic activity of graphite.	10.26%	The DSSC Pt + tri-carbon has high PCE due to the bottom cell's full usage of transmitted light. The J_{sc} and FF were close to 20 mA/cm^2 and 73.33, respectively, with a parallel mode used.
Zheng *et al.*, (2015)	A counter-electrode (CE) for dye-sensitized solar cells (DSSCs) was prepared by coating a slurry containing acid-oxidized multi-wall carbon nanotubes and nano-graphite powder onto a fluorine-doped tin oxide conducting glass substrate.	4.10%	Results show that the cell with the CE exhibits the best photoelectric properties of all the carbon-based CEs investigated. The short-circuit current density (J_{sc}) is 4.67 mA/cm^2, the open-circuit voltage (V_{oc}) is 0.53 V and photoelectric conversion efficiency is up to 4.10%, which are comparable with those of the Pt-based CE in DSSCs.

Materials and Methods

Materials for Dye Sensitized solar cells are:

- Fluorine doped tin oxide (FTO) glass 10cm x 10cm (15Ω/m^2)
- Blocking layer (compact layer TiO_2)
- Oxide film (mesoporous TiO_2)
- Sensitizer (dye)
- Counter-electrode (Pt/MWCNT, MWCNT and Elcocarb).
- Iodide/triiodide (electrolyte)

Methods

Preparation of Counter-electrode

- Catalyst Preparation
- Carbon Nanotube Production
- Purification and functionalization of CNTs produced
- Preparation of Pt-MWCNT
- Development of Electrode (Counter-Electrode)

Catalyst production

2^3 factorial experimental design was used for optimisation of synthesis parameters on Fe-Co/$CaCO_3$ bimetallic catalyst.

2.47 g mass of $Co(NO_3)_2.6H_2O$

and

3.62 g mass of $Fe(NO_3)_3.9H_2O$

+

8-10 g of $CaCO_3$ all in 50 ml of distilled water.

To age for 60 minutes under constant stirring on magnetic stirrer until it become a gel.

Baked between 100 °C and 120 °C for 8 or 12 hours.

Cool to room temperature

Screened through 150µm sieve into fine powder.

Calcined at 400 °C for period of 16 hours in a furnace.

Results and Discursions

Catalyst

Table 1: 2^3 Experimental Matrix showing Yield after Drying and Calcined at 400 ^{0}C

Run	Mass of Support (g)	Drying Temperature (°C)	Drying Time (hrs)	Yield (%) After Drying	Yield (%) After Calcination at 400 ^{0}C
1	10	100	8	76.50	86.69
2	8	120	12	67.25	76.79
3	10	120	8	77.50	85.31
4	8	120	8	82.25	78.00
5	8	100	8	76.00	85.10
6	10	120	12	78.75	95.71
7	10	100	12	70.25	86.45
8	8	100	12	74.00	84.60

CHARACTERIZATIONS OF CATALYST

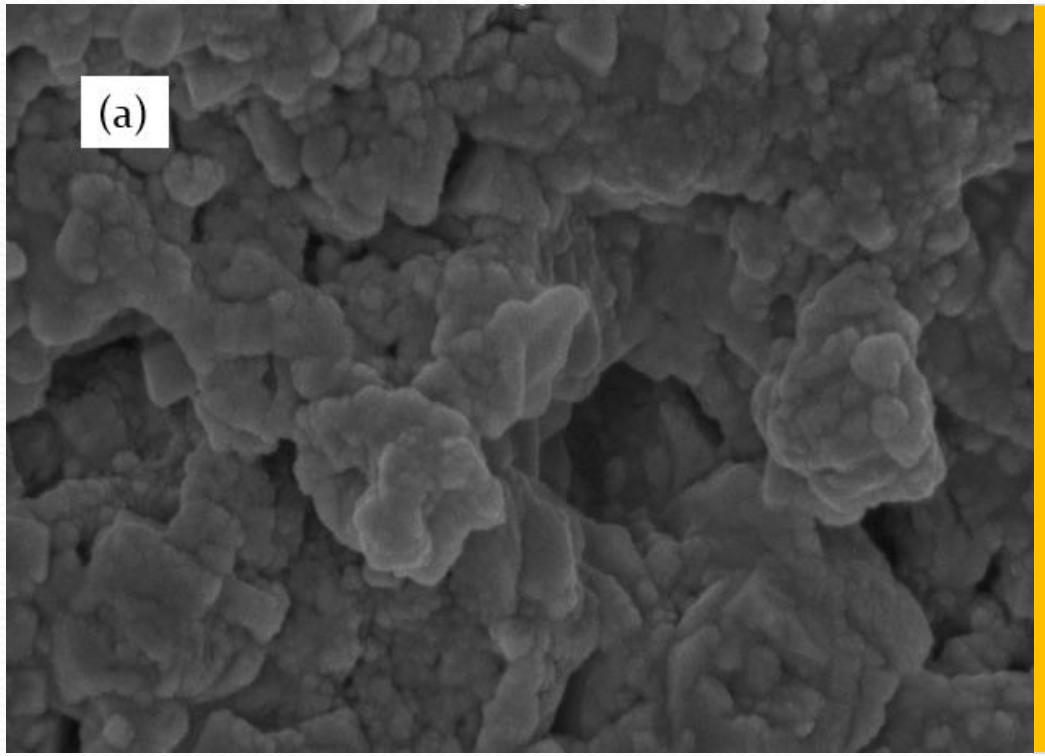

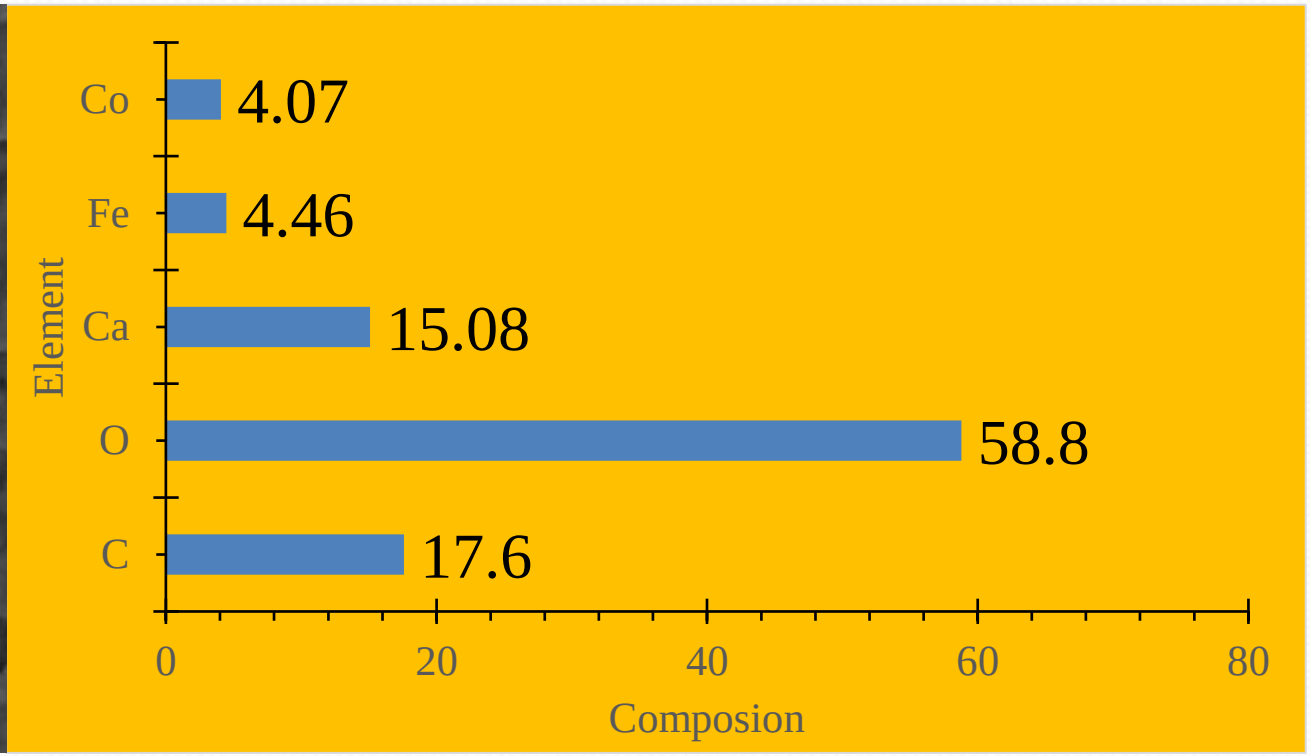

Figure 1: (a) SEM image showing nanoparticles of Fe and Co dispersed on $CaCO_3$ support and (b) **EDS elemental compositions of catalyst sample**

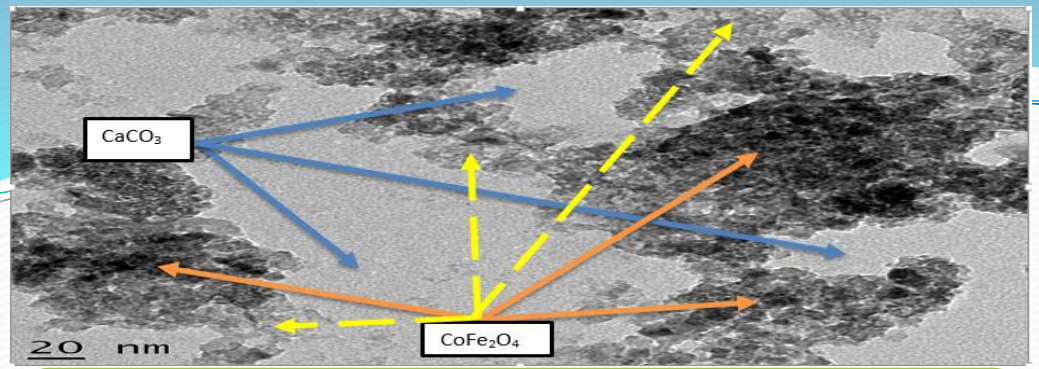

Figure 2: HRTEM images of the catalyst showing a clear view of coloured metal ions; (light brown Fe^{3+}, dark/black Co^{2+}) and white $CaCO_3$ bulk with modified crystal morphologies.

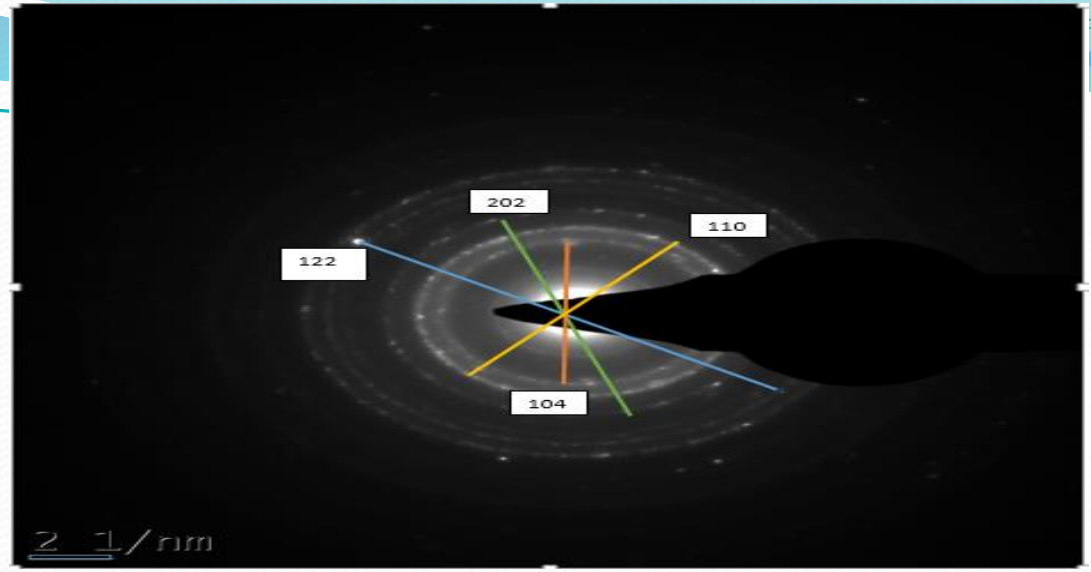

Figure 3: SAED of the Fe-Co/$CaCO_3$ catalyst showing sharpest rings of $CaCO_3$ at (104) plane.

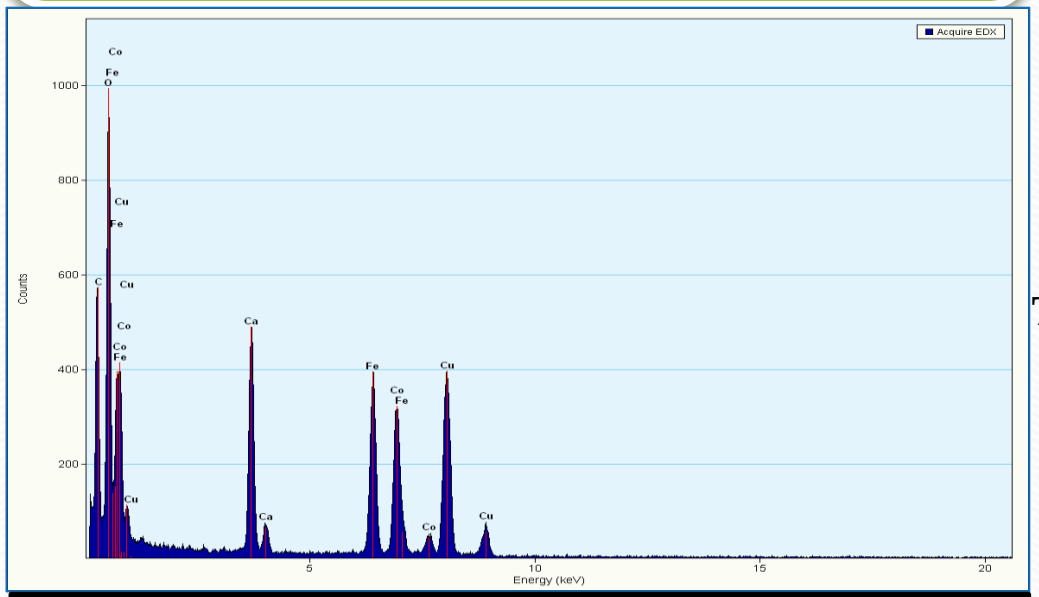

Figure 4: TEM/EDS of the Fe-Co/$CaCO_3$ catalyst

Table 2: Rhombohedral $CaCO_3$ phase identification in SAED pattern

2θ (°)	1/d (1/nm)	d (nm)	d (Å) (SAED)	d (Å) (XRD)	d (Å) (Literature)	hkl
29.4163	6.5907	0.3035	3.0346	3.0329	3.0357	104
35.9800	8.0349	0.2489	2.4891	2.4933	2.4950	110
43.1753	9.5911	0.2085	2.0853	2.0930	2.0946	202
57.4286	12.2853	0.1628	1.6280	1.6031	1.6042	122

(Woodward and Amjad, 2014; Downs et al., 1993)

Reference: (Amjad, 2014; Downs *et al.*, 1993)

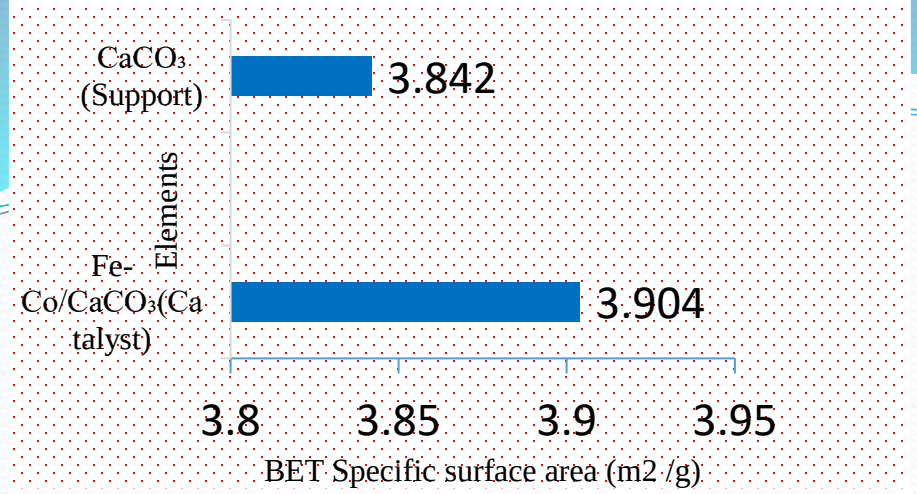

Figure 5: Surface area of $CaCO_3$ and Fe-Co/$CaCO_3$ catalyst

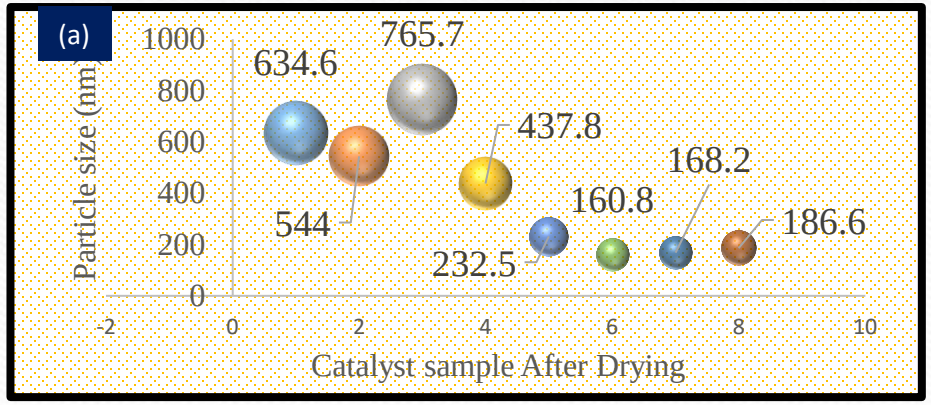

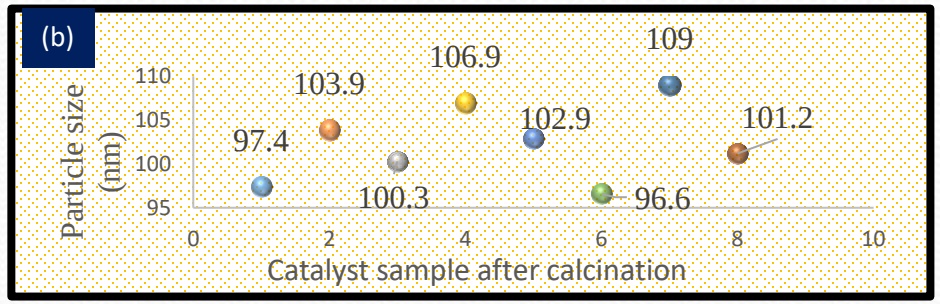

Figure 6 (a) and (b): Catalyst particle sizes after drying at 120 °C calcination at 400 °C

Figure 5: Specific surface area of catalyst was found to be 3.904 m²/ g while $CaCO_3$ used as support possessed specific surface area of 3.842 m²/ g (Mhlanga *et al.*, 2009).

No significant change in surface area because there is no thermal decomposition of the major catalyst component, $CaCO_3$, occurred at the treatment temperature of 450 °C (Al-Fatesh and Fakeeha, 2012).

Dispersion of Fe and Co nanoparticles in the support matrix is attributed for the slight increase in surface area.

Catalyst has specific pore volume of about 0.002 cm³/g, and pore radius of between 0.184 and 1.4 nm

Figure 6: DLS before and after calcination shows that the catalyst sample particles were in the ranges from 160.8-765.7 nm and 96.6-109.0 nm respectively.

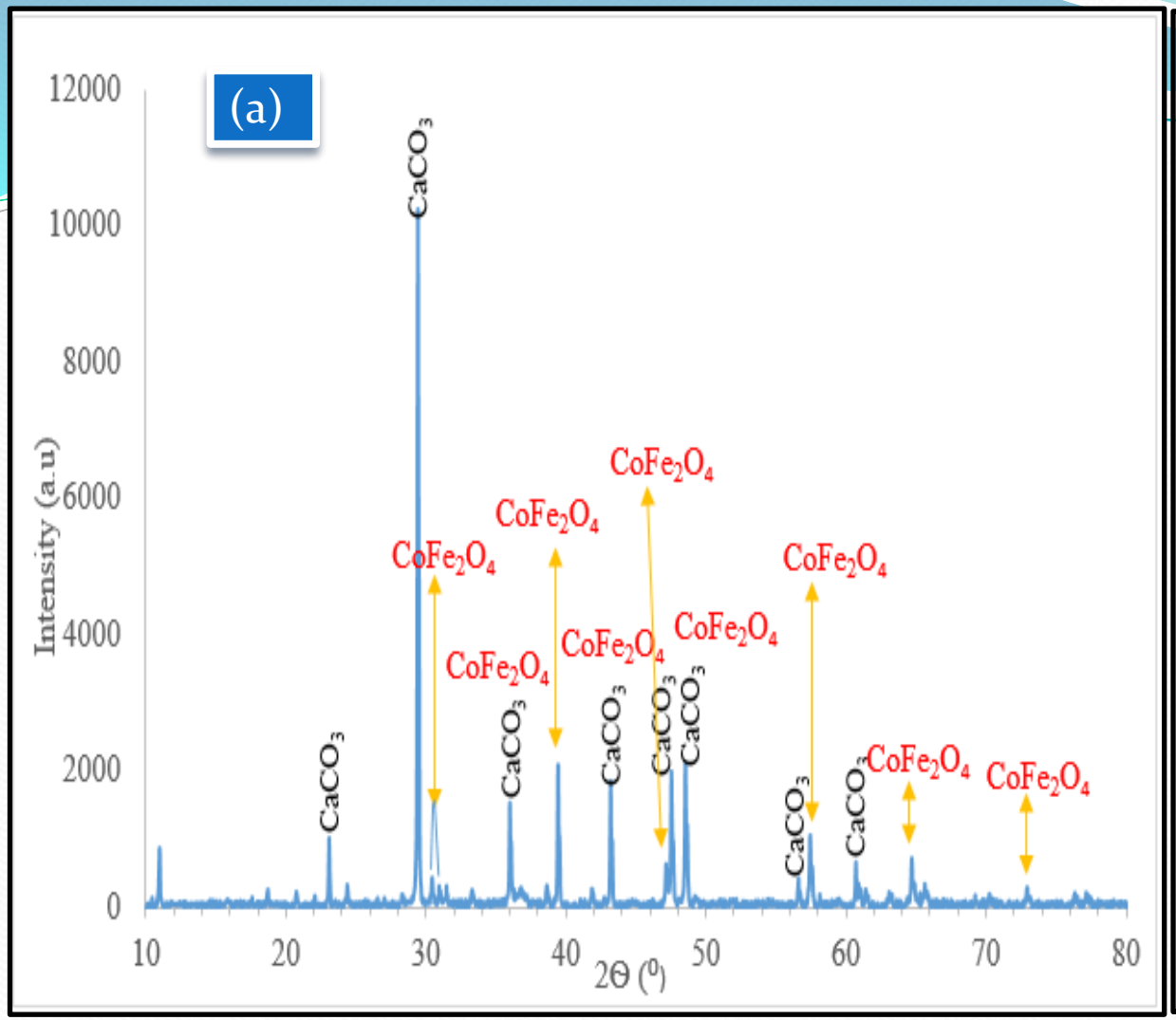

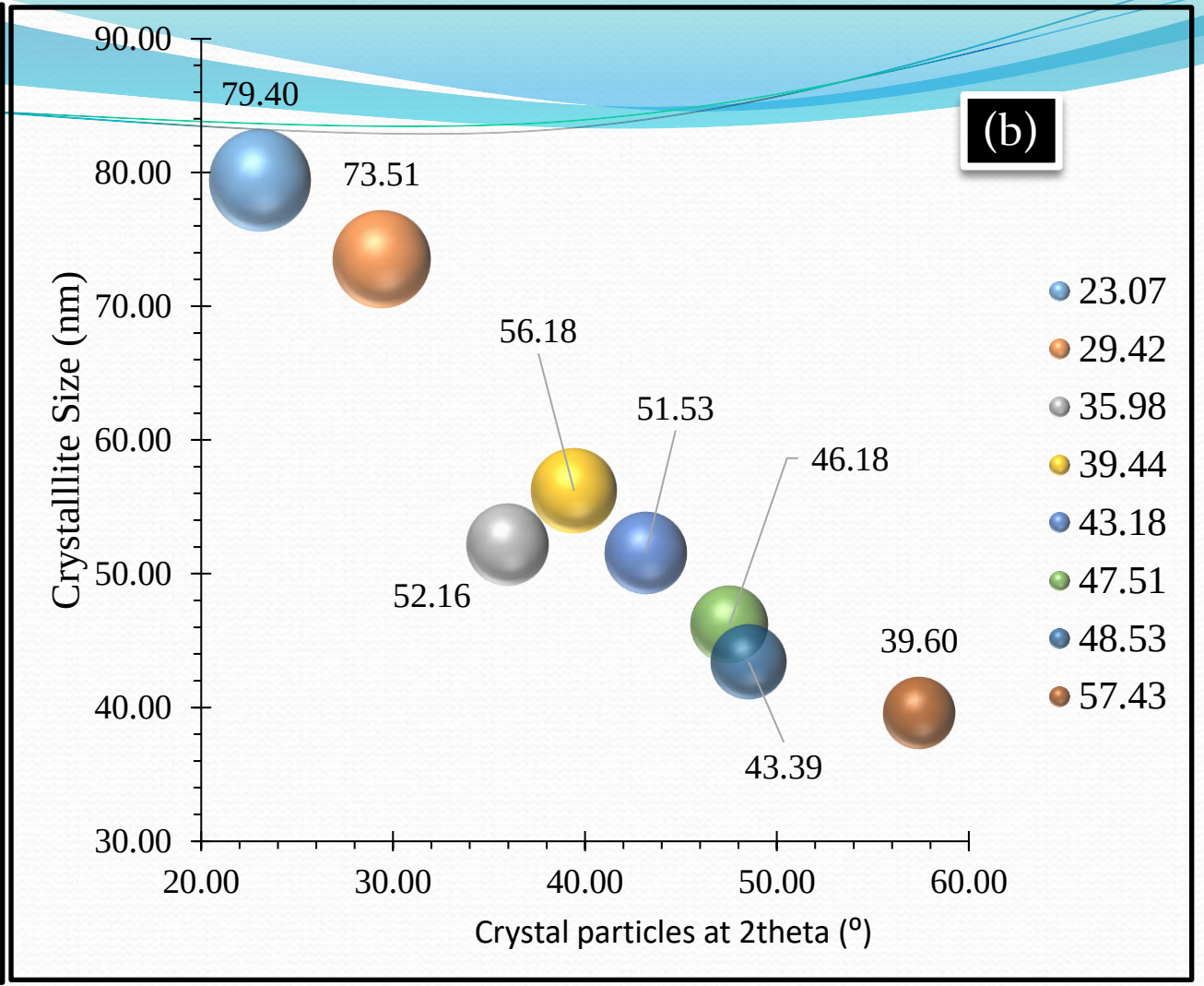

Figure 7: XRD pattern of Fe-Co/$CaCO_3$ catalyst showing (a) phases of $CaCO_3$ and $CoFe_2O_4$, (b) Polycrystalline particles with sizes ranging from 39.6 nm to 79.4 nm

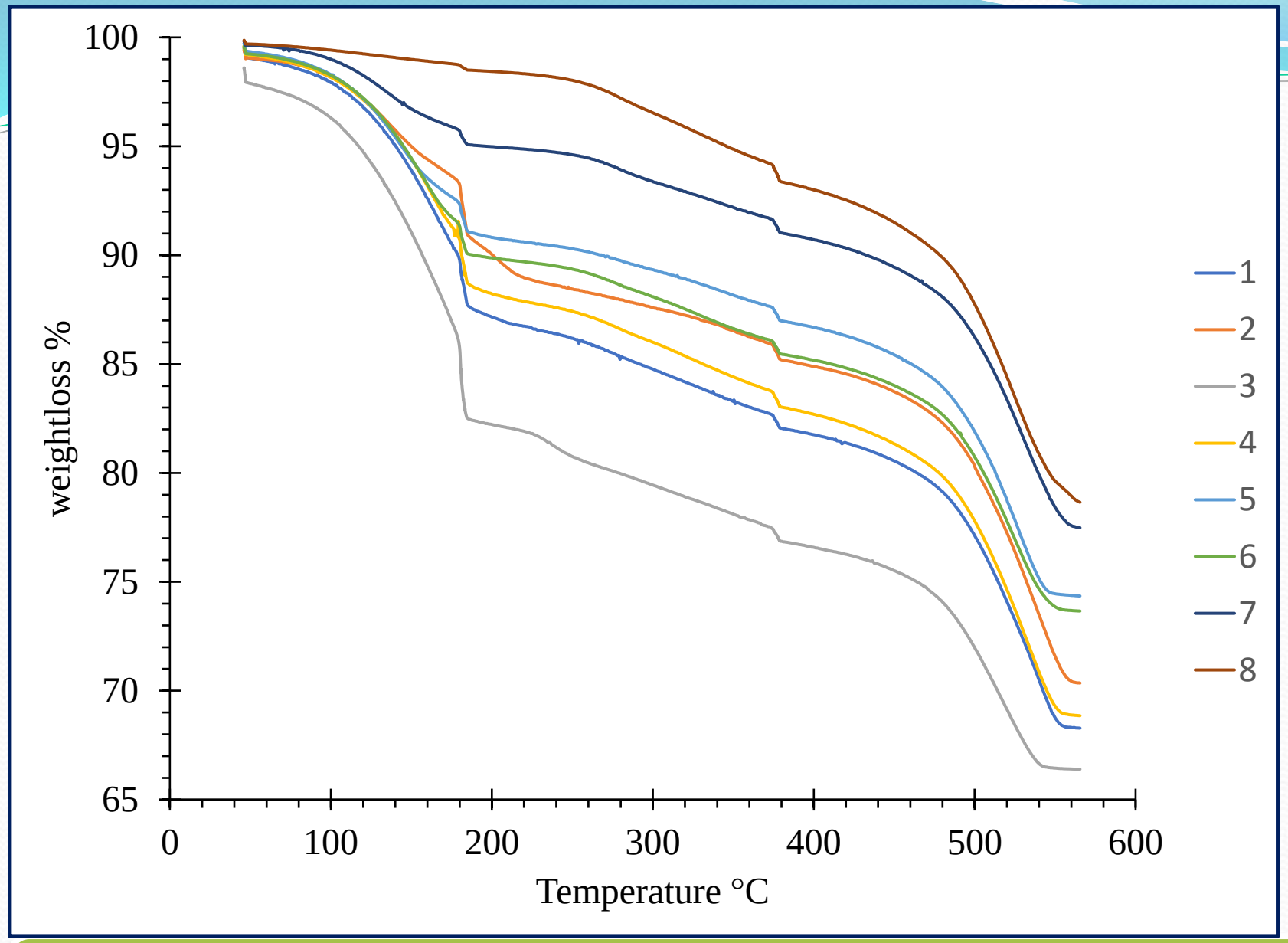

SAMPLE ID	Weightloss (%)
1	31.72
2	29.65
3	33.61
4	31.15
5	25.65
6	26.35
7	22.51
8	21.35

Figure 8: The thermal decomposition curve of the Fe-Co/$CaCO_3$ catalyst

Synthesis of carbon nanotubes

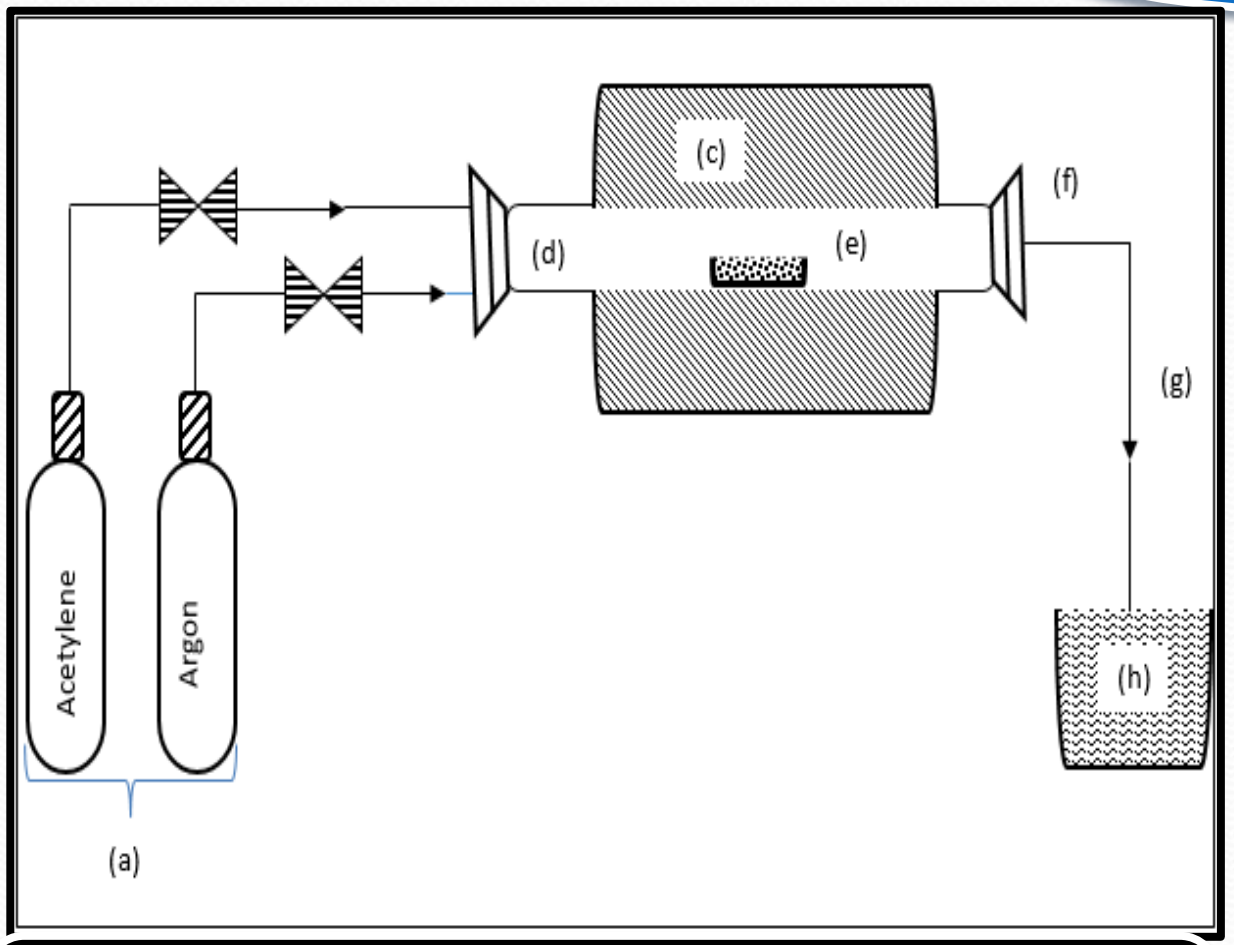

Figure 9: Schematic diagram of experimental set-up for CNT synthesis in CVD

Mass of catalyst	0.5 g
Heating rate	10 °C min^{-1}
Initial argon flow rate	30 ml min^{-1}
Reaction temperature	700 °C
Acetylene flow rate	290 ml min^{-1}
Final argon flow rate	190 ml min^{-1}
Reaction time	60 min

(a) CNTs +acid in ratio 3: 1 (H_2SO_4:HNO_3) to remove metallic impurities

(b) Sonicate for 3 hours at 45 °C temperature to enhance metal dispersion

(c) Washing with distilled water to a pH of 7

Dried in the oven at 120 °C for 12 hours & CNTs

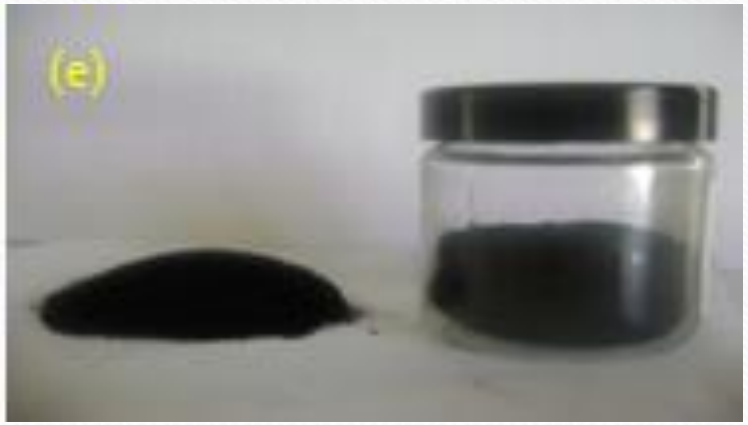

Plate(s) 1 (a) to (e): Purification process of Carbon Nanotubes (CNTs)

CNTs

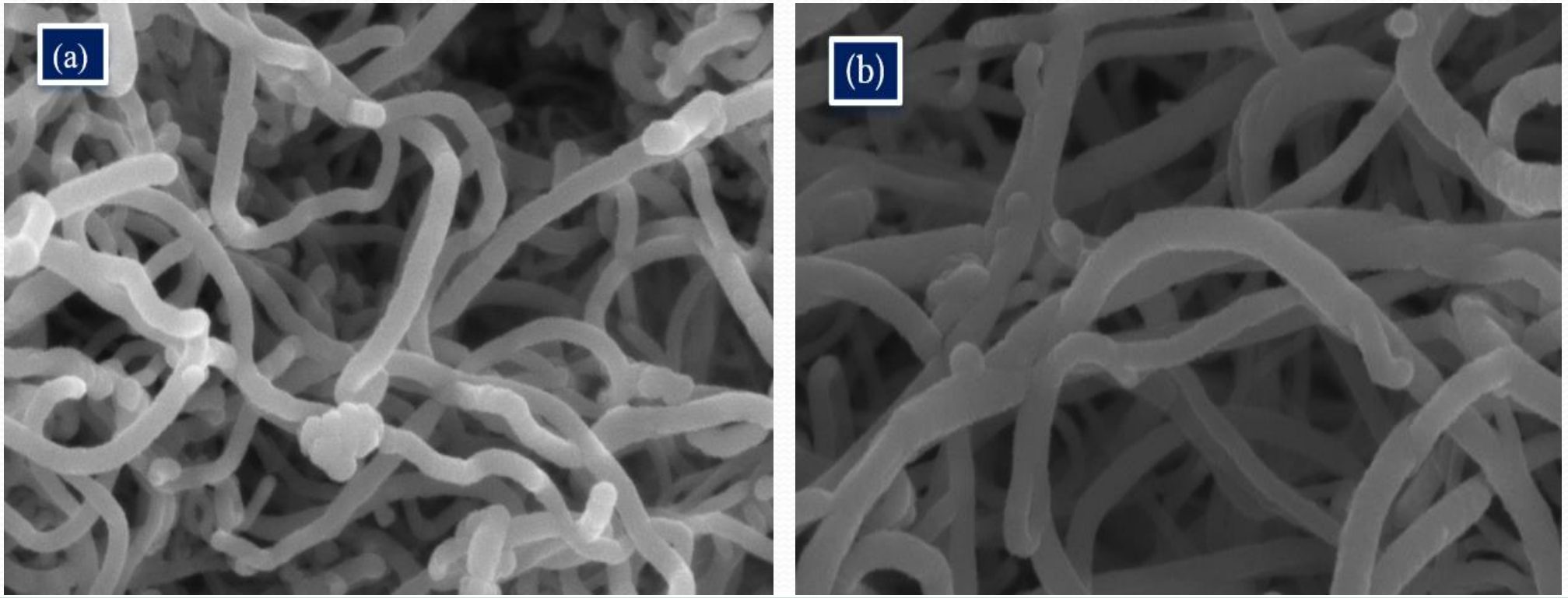

Figure. 10: is SEM image (a) exhibits a slight degree of agglomeration with some bright spots, which corresponds to the residual metal particle from catalyst metal particles, support materials, and amorphous carbon on the surface of CNTs while (b) exhibit a clear defined tubular morphology (nodules like structure).

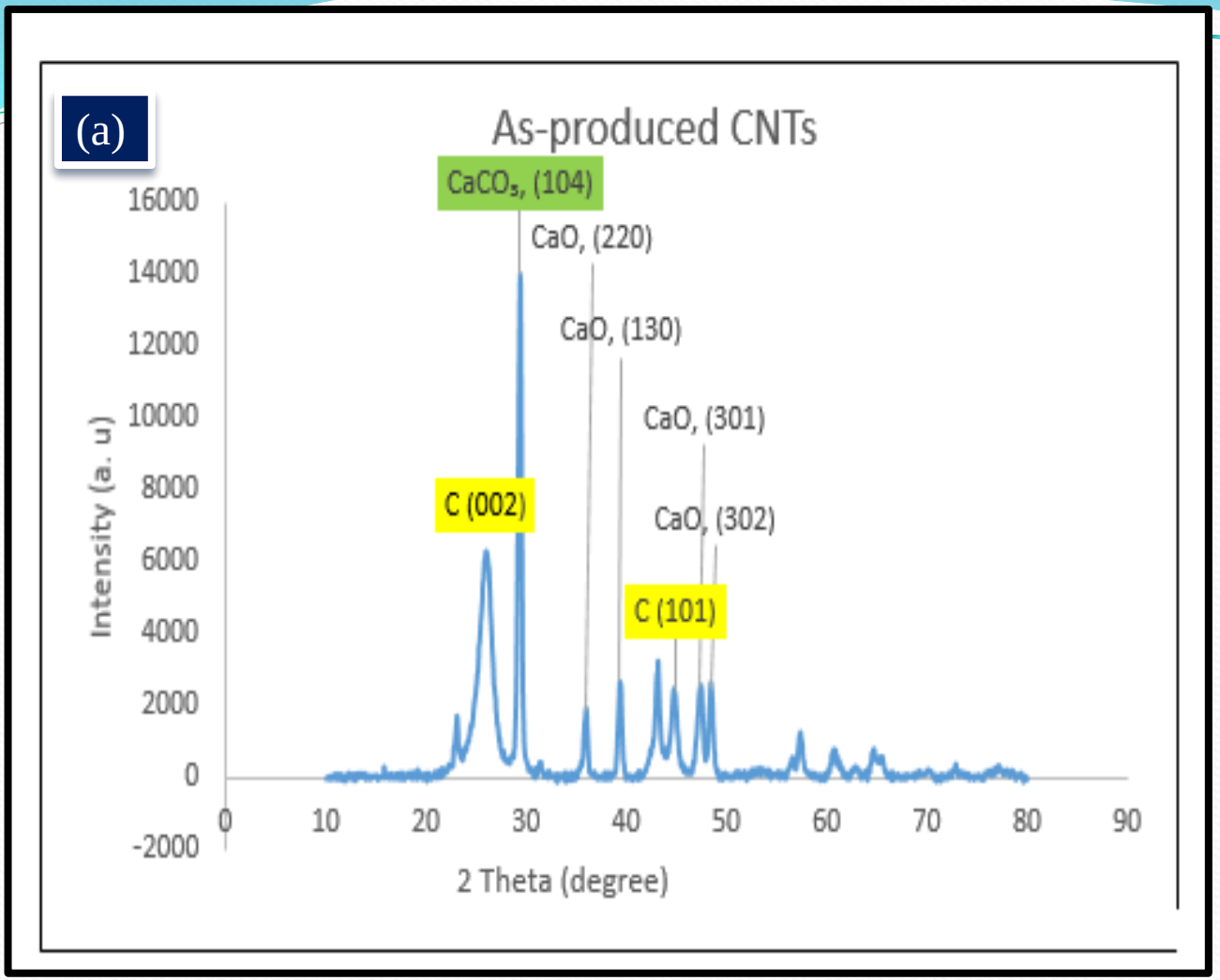

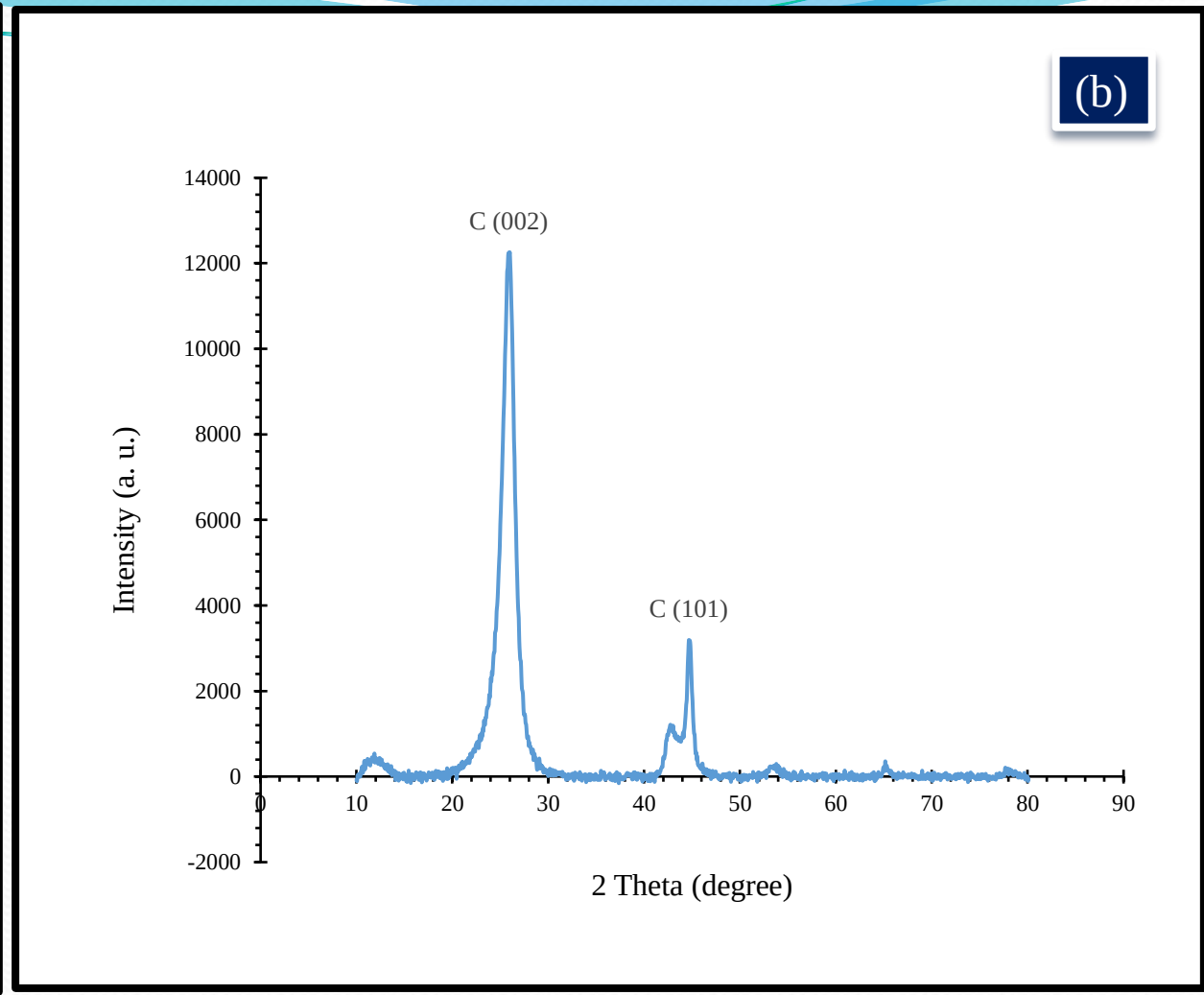

Figure 11: XRD pattern of (a) as-produce and (b) purified. The crystallite sizes range from 5.64 nm to 32.24 nm and 1.8 nm to 12.10 nm respectively

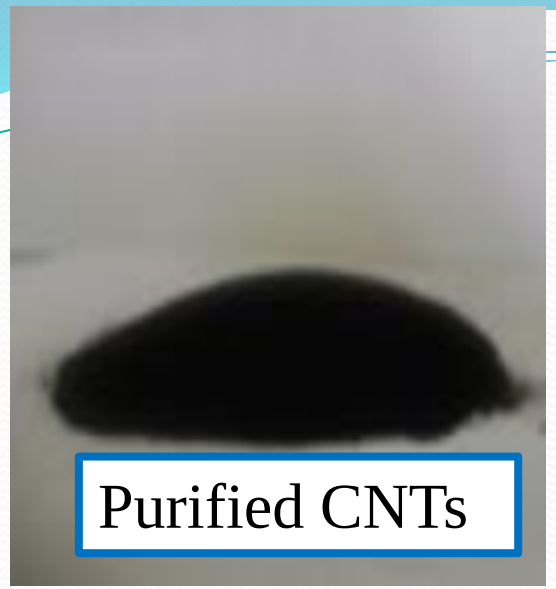

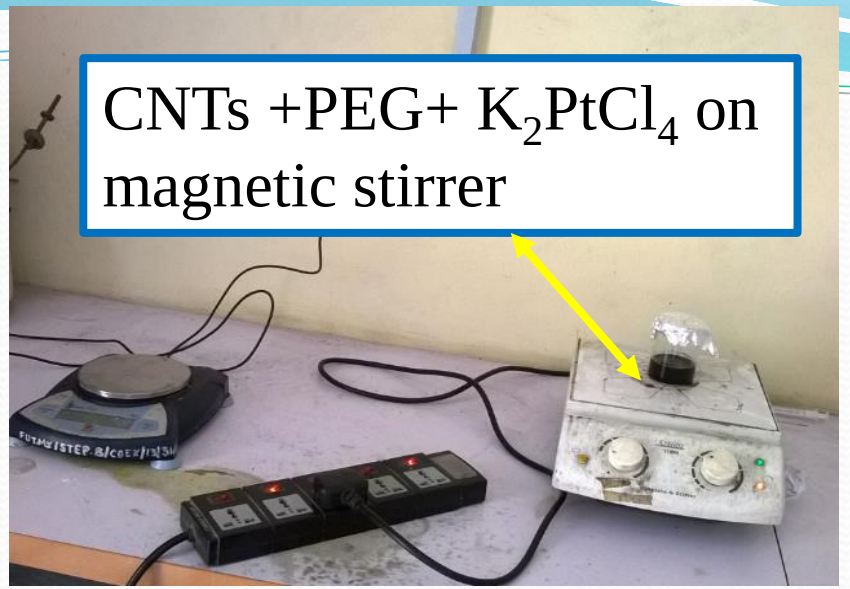

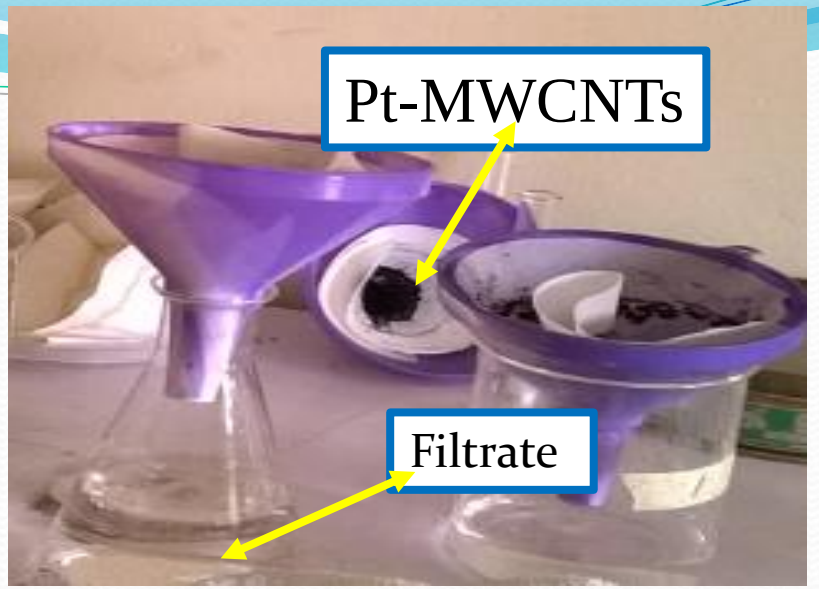

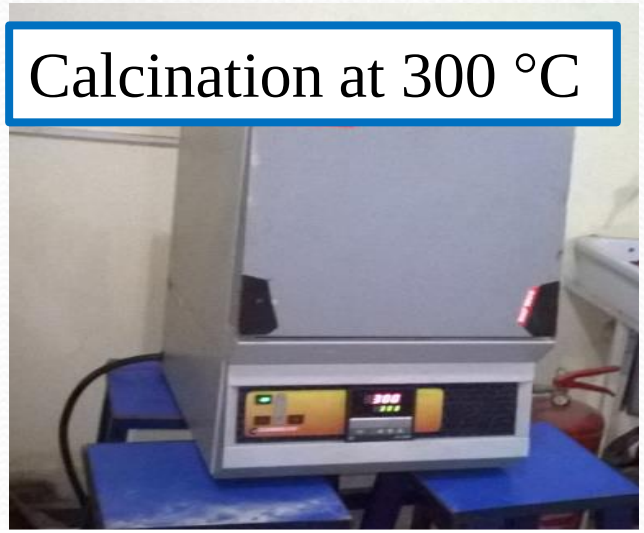

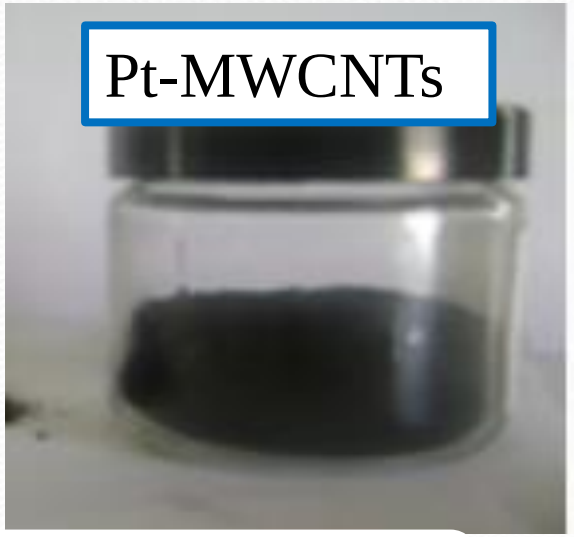

Plate 2 : Preparation procedure of Pt-MWCNTs

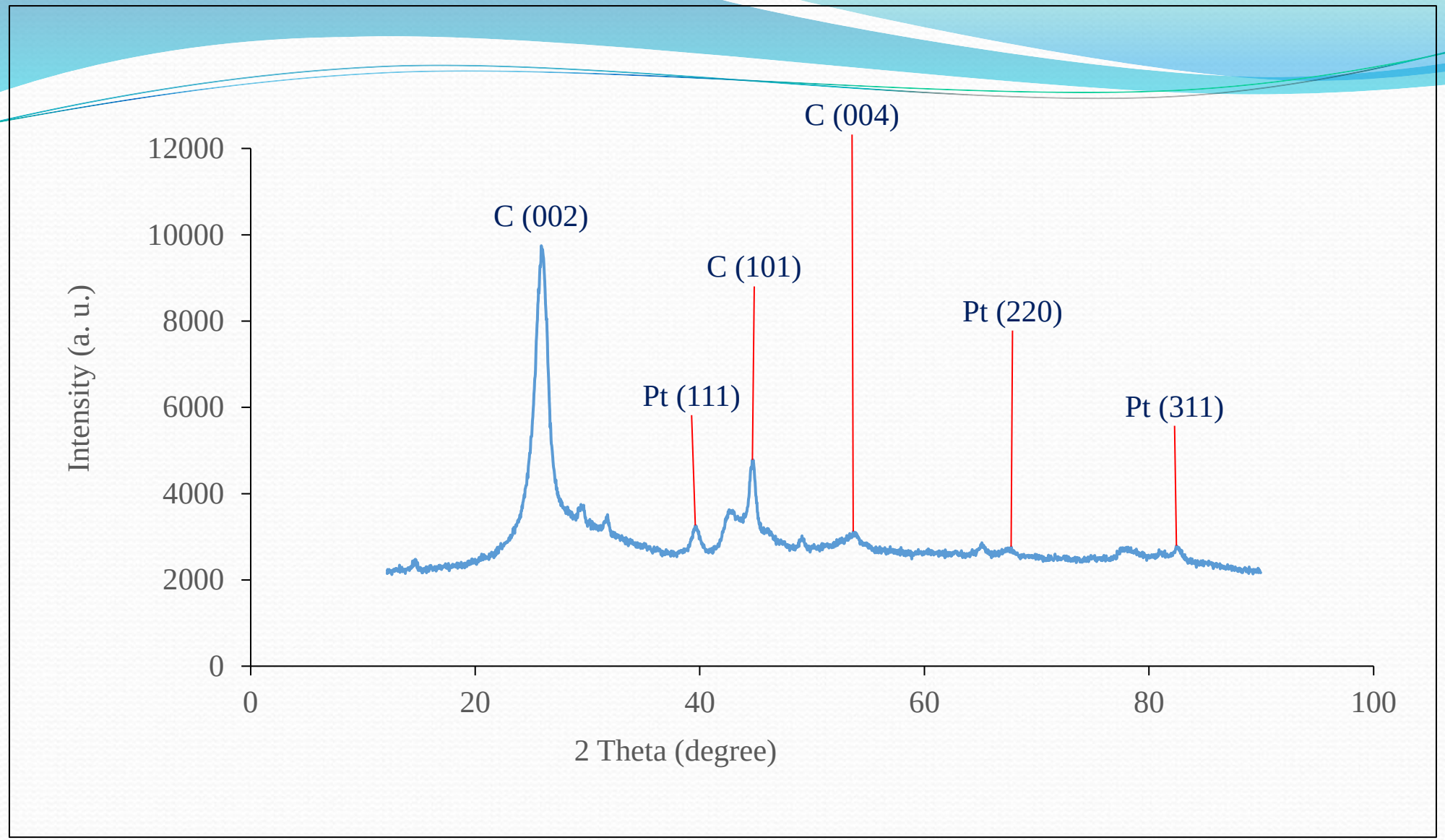

Figure 12: (a) XRD pattern of Pt-MWCNTs. Major diffraction peak was found to be Pt (111) at 2 theta of 39.60. with crystallite size of 1.35 nm.

Pt-MWCNTs

Table 3: UV Analysis showing Pt percentage concentration on CNTs

Dispersion time (mins)	Absorbance (a.u)	Filtrate Concentration	Concentration of Pt on CNTs	% Concentration of Pt on CNTs
270	0.887	3.52	0.65	15.54
300	0.854	3.37	0.79	19.05
330	0.772	3.01	1.16	27.79
360	0.751	2.92	1.25	30.03
390	0.722	2.79	1.38	33.12
420	0.708	2.72	1.44	34.62
450	0.689	2.64	1.53	36.64
480	0.665	2.53	1.63	39.20

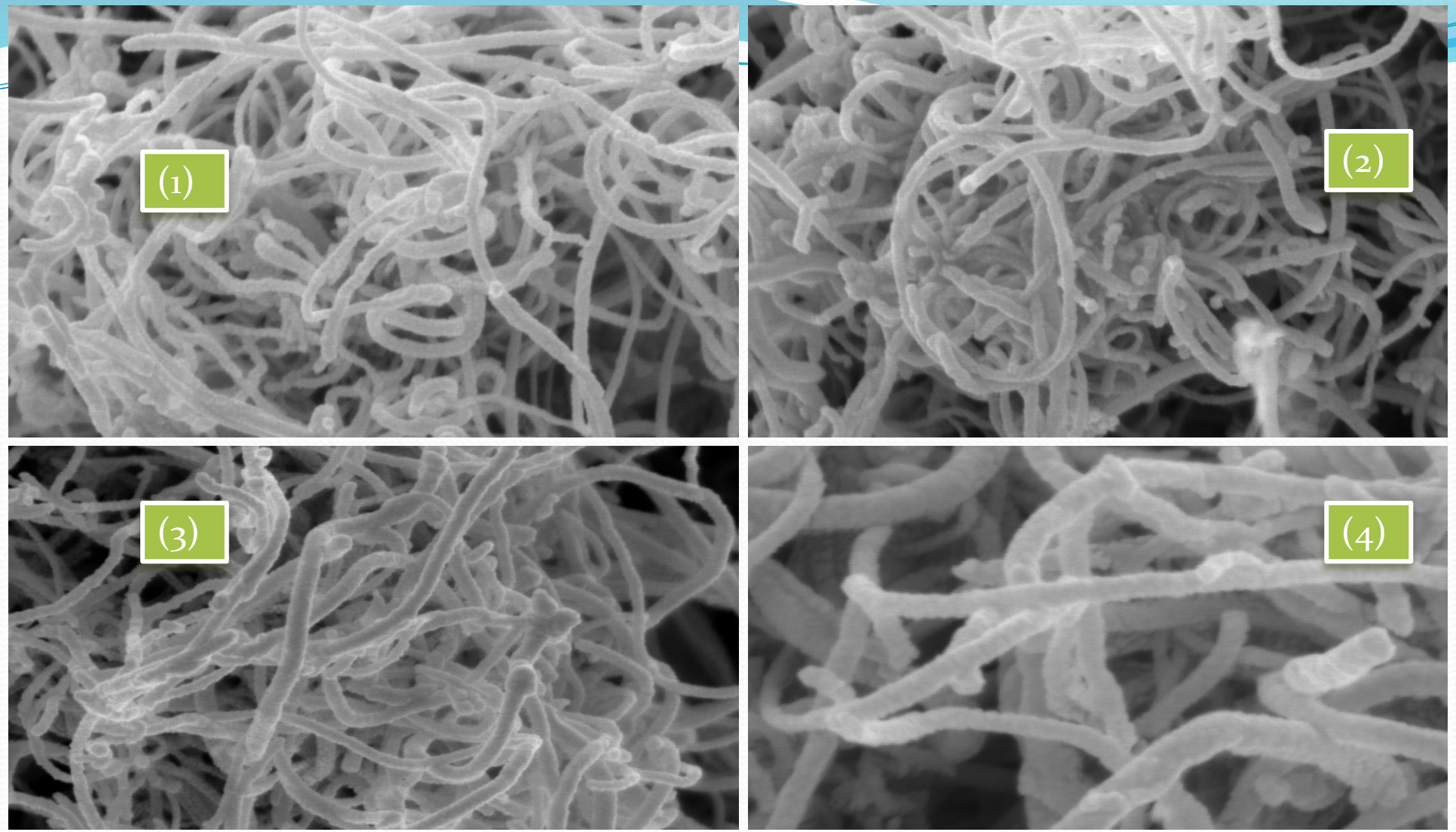

Figure 13: SEM Images (1) to (4) Showing Effect of Pt % concentrations from (15.54 %) to (30.03 %) on MWCNTs respectively.

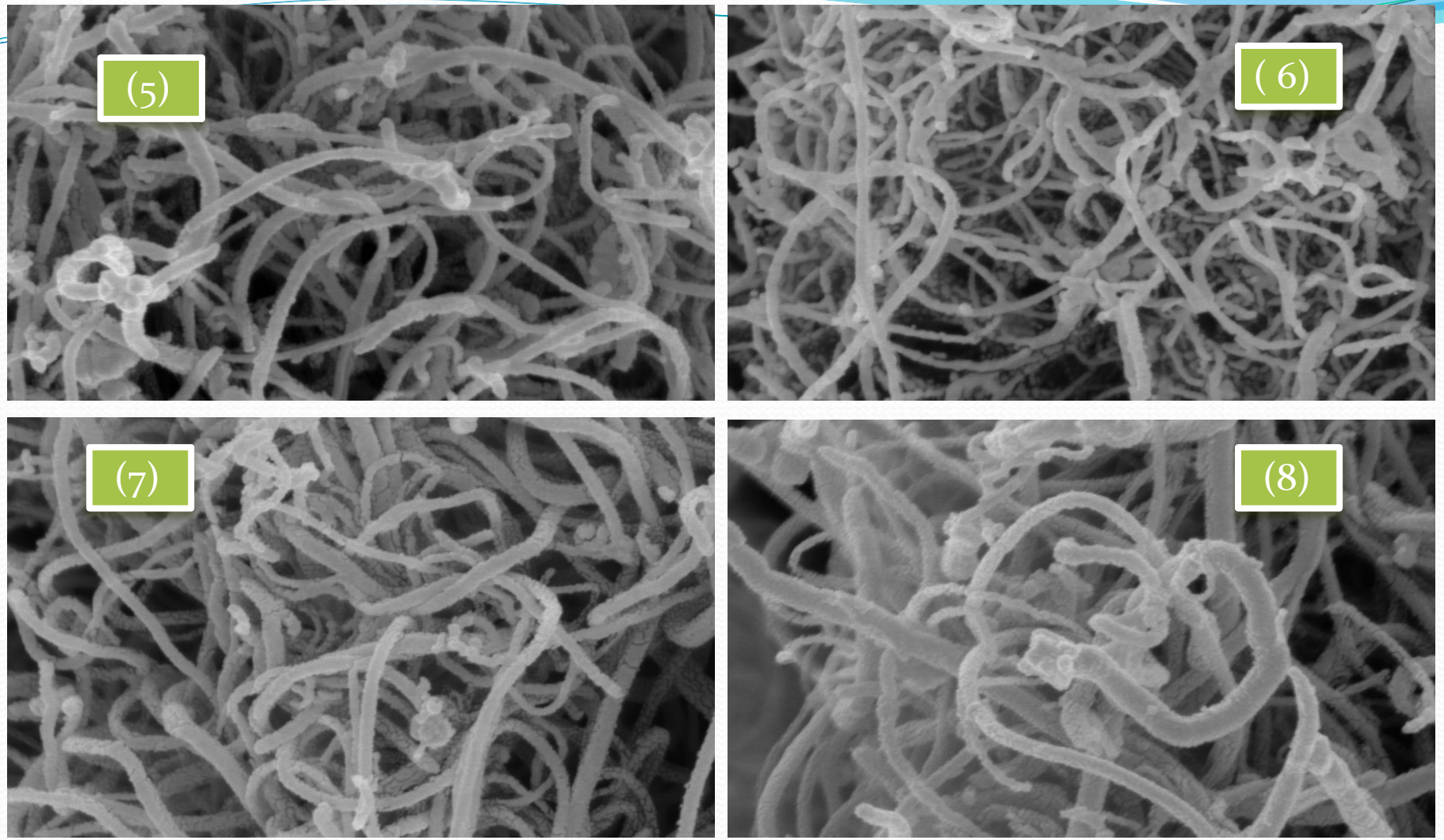

Figure 14: SEM Images (5) to (8) Showing Effect of Pt % concentrations from (33.12 %) to (39.20 %) on MWCNTs respectively.

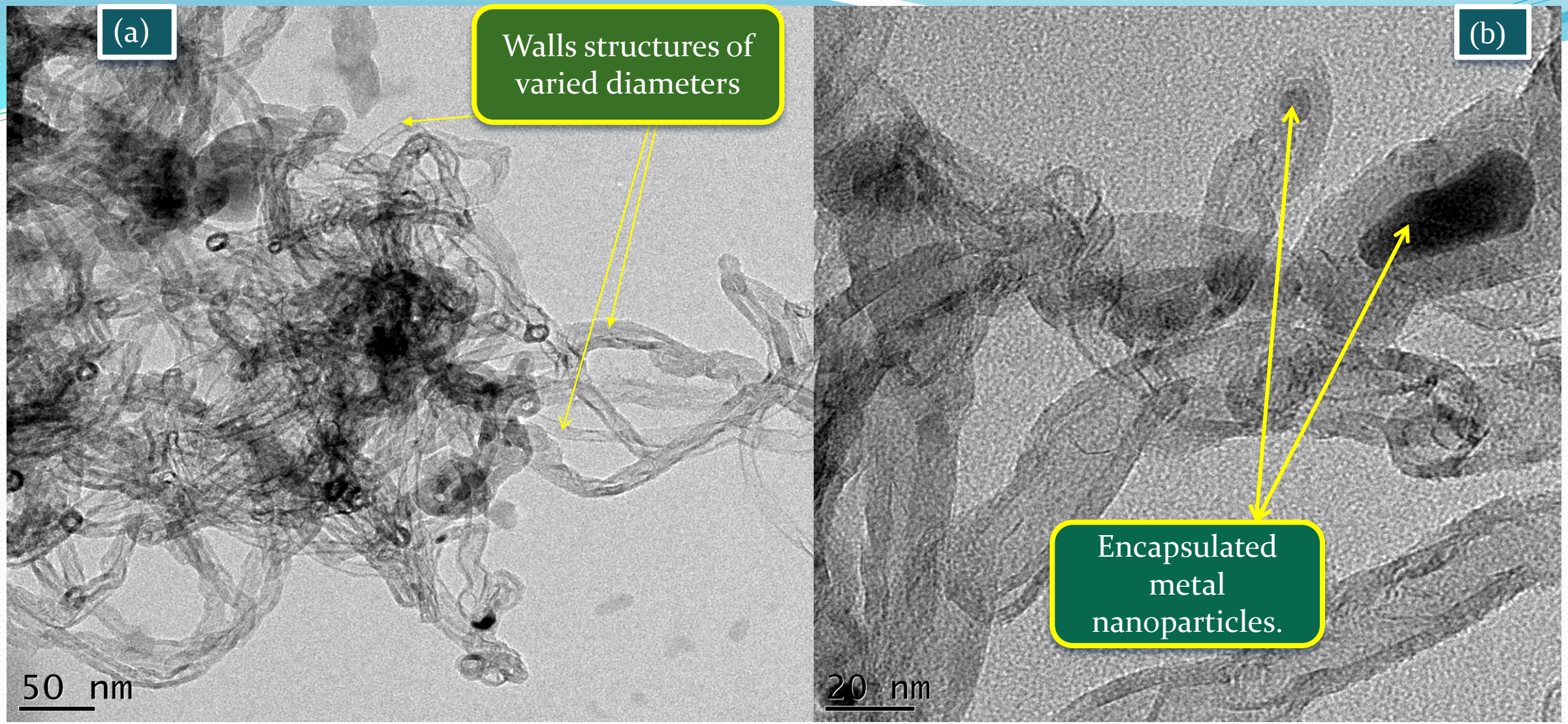

Figure 15: TEM images of (a) as-produced MWCNTs and (b) purified CNTs showing encapsulated metal nanoparticles along the inside diameter. Wall structures vary and their diameter distribution are not the same

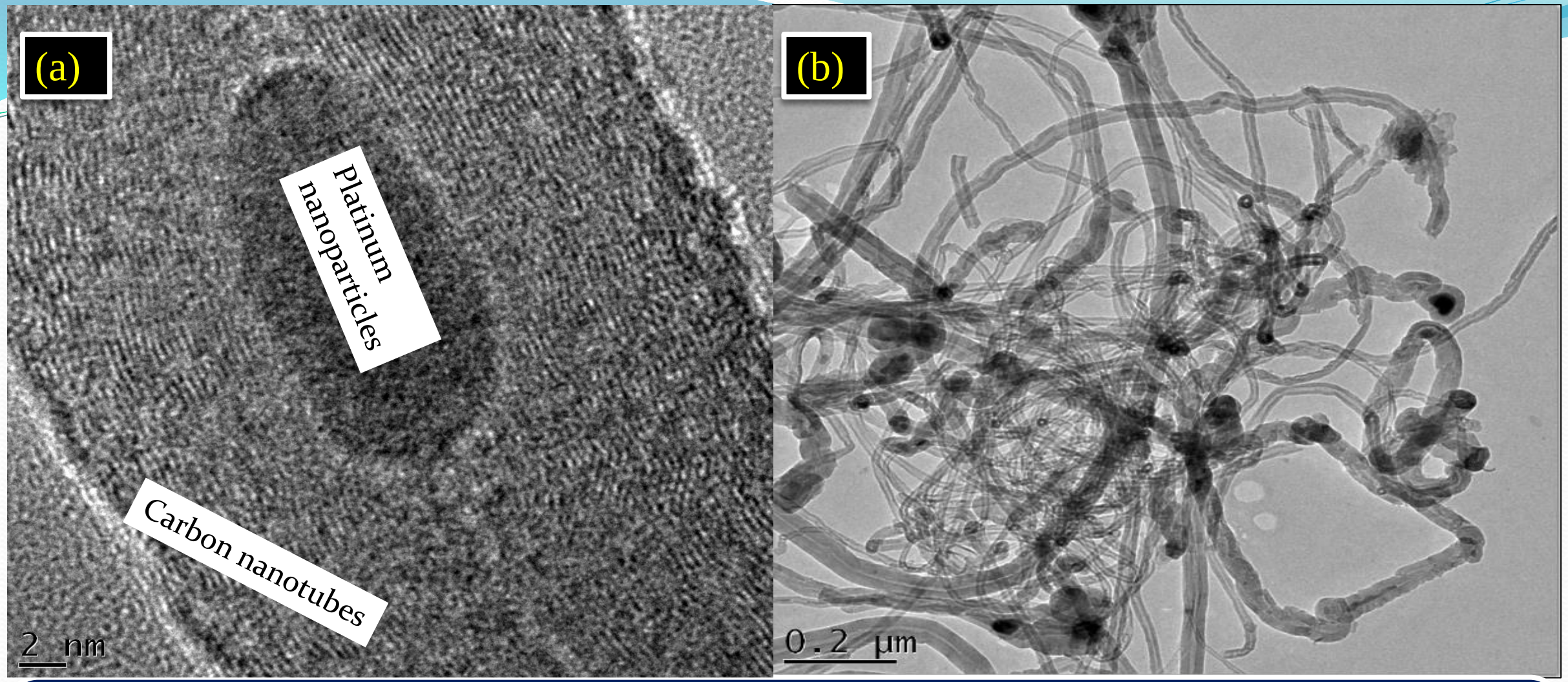

Figure 16: (a) showing evidence of Pt. catalyst on the nanotube, (b) showing evidence of tubes of different diameters with Pt nanoparticles evenly distributed on the outer surface of the tubes.

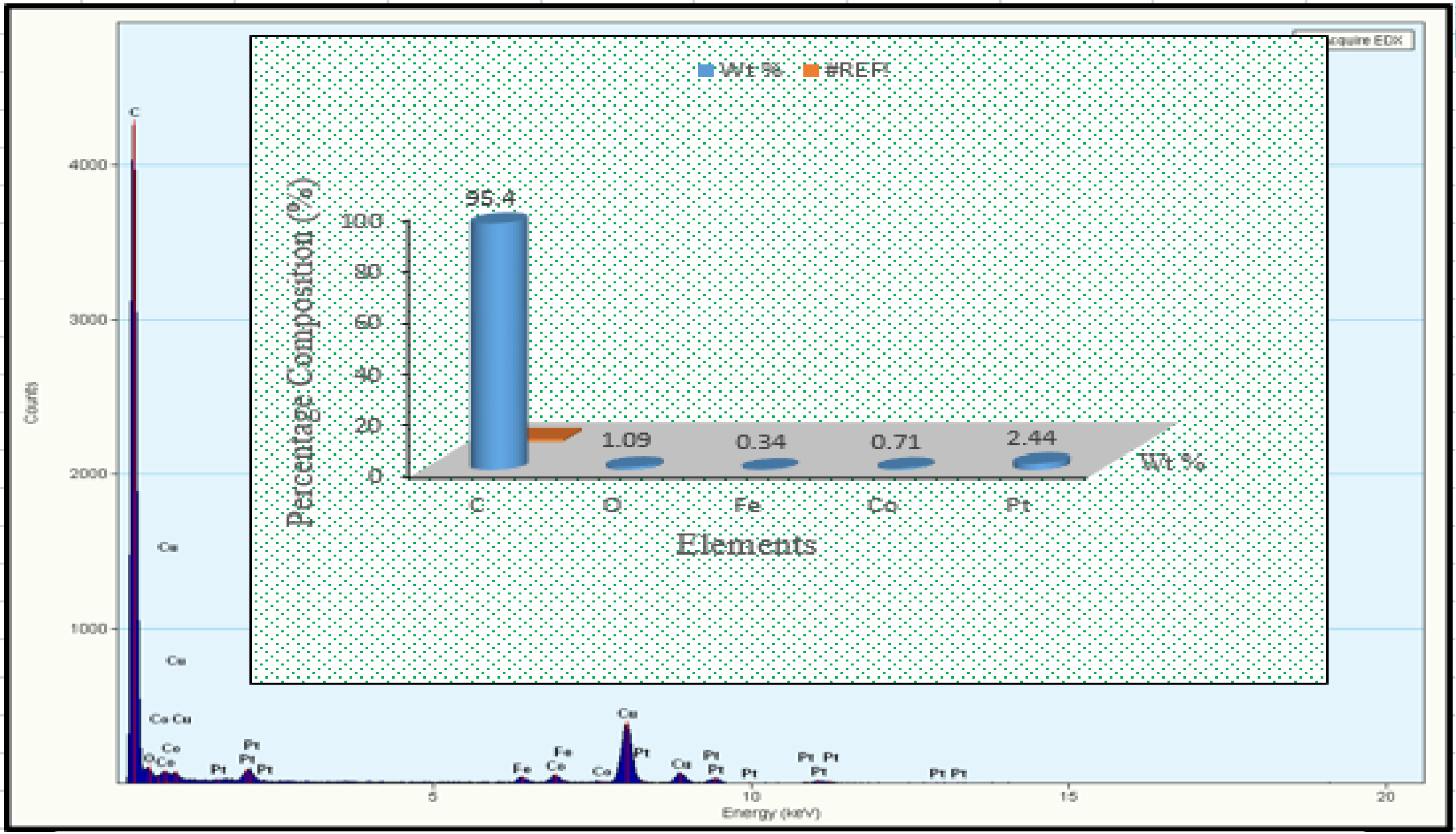

Figure 17: TEM/EDX analysis of the Pt–MWCNT catalyst sample confirming the presence of Pt.

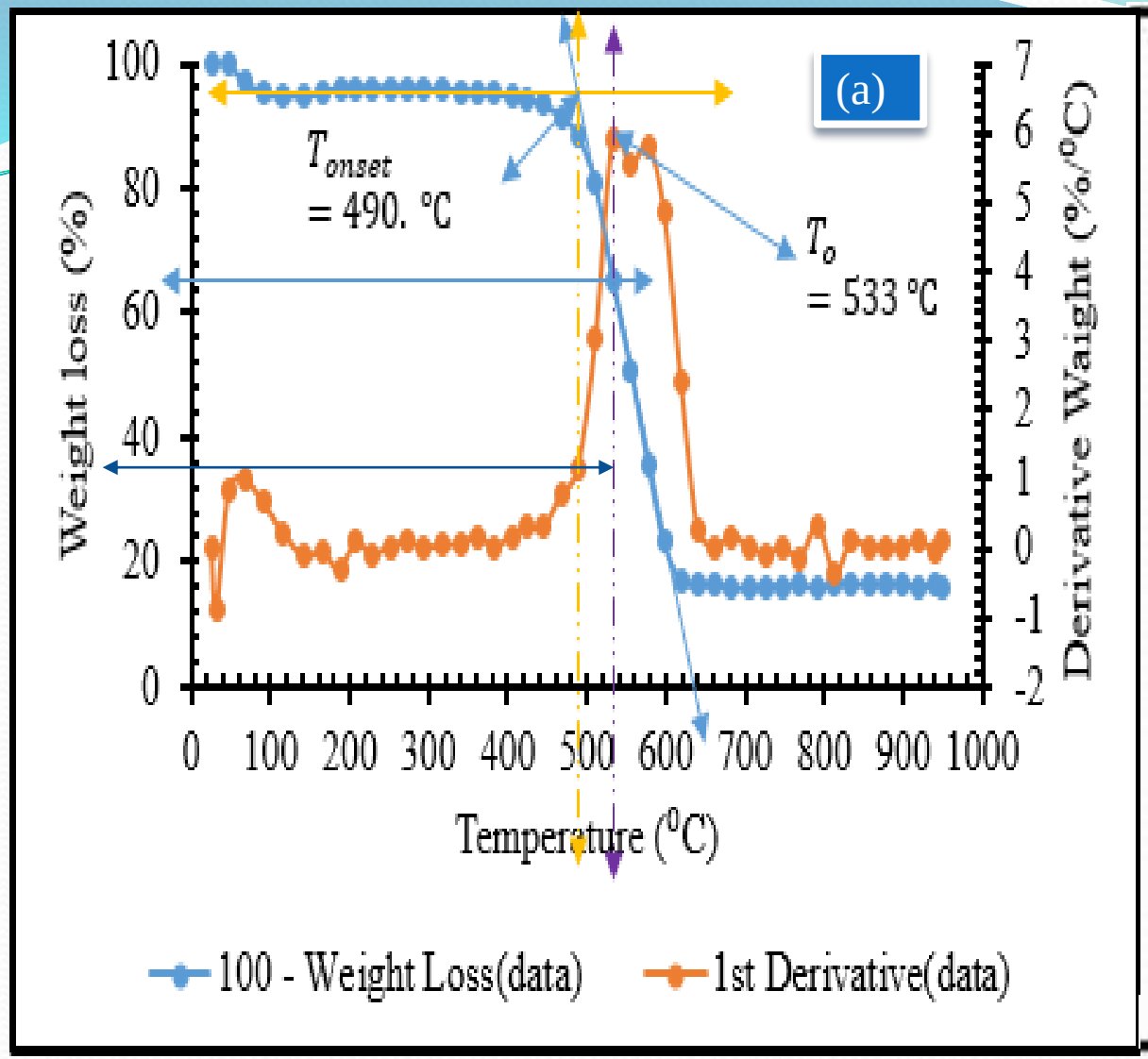

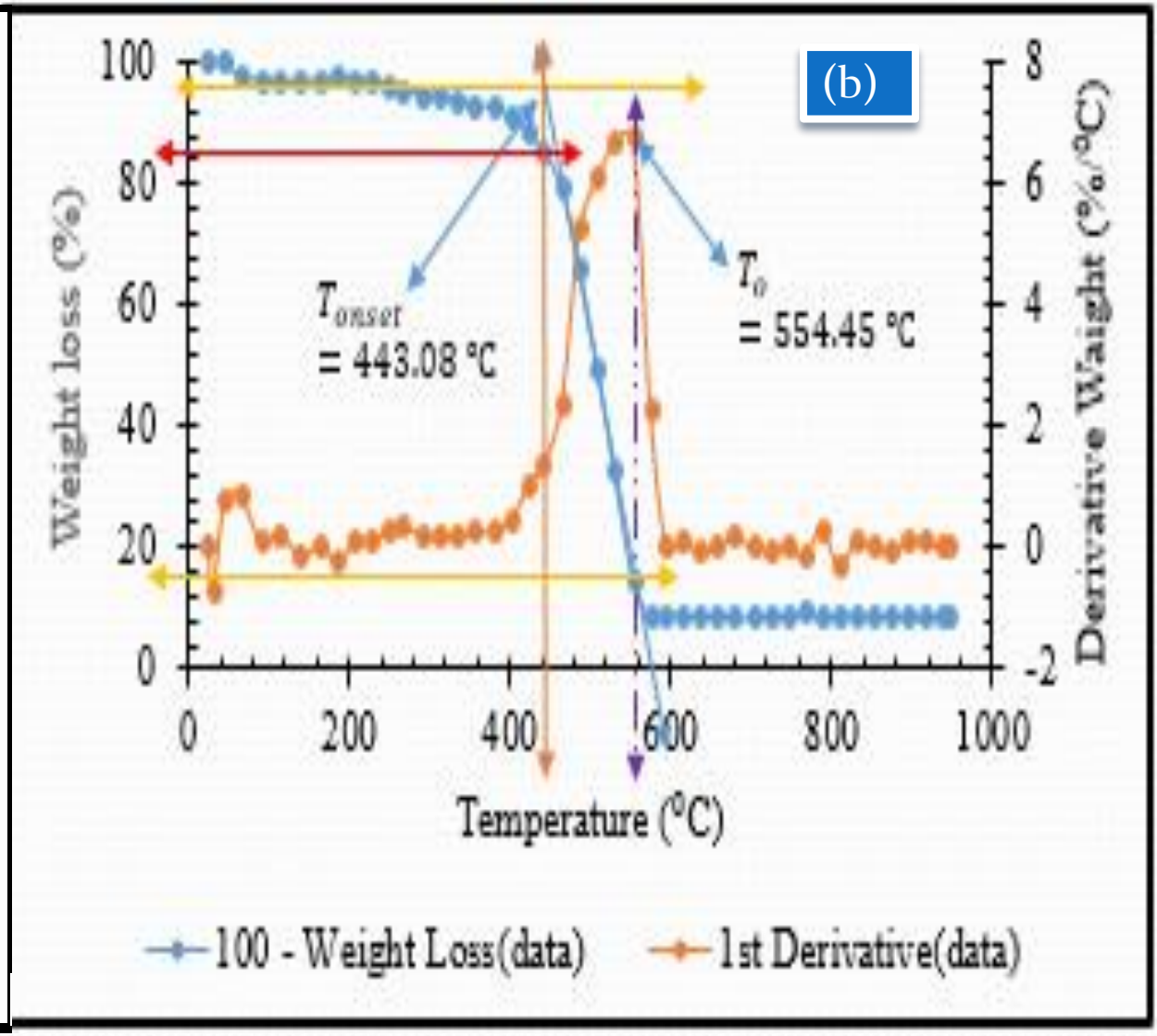

Figure 18: is the TGA/DTG curves of (a) purified and (b) functionalised MWCNTs with the weight loss of about 34.87 % and 85 % respectively.

Table 4: BET analysis of As-produced, Purified and Pt-MWCNTs catalyst samples

MWCNTs.	Surface area (m^2g^{-1})	Pore volume (cm^3g^{-1})
As-produced	272.98	62.72
Purified	274.06	62.97
33.12 wt% Pt. (Pt-MWCNTs)	**432.6**	**19.14**
34.62 wt% Pt. (Pt-MWCNTs)	**609.2**	**26.82**
39.20 wt% Pt. (Pt-MWCNTs)	**858.7**	**38.82**

Ultrasound process breaks the CNTs agglomerates and resulting in more separate CNTs in the same mass and volume, thus more surface area.

FABRICATION OF DSSCs

- Cleaning and Preparations of FTO glass
- Deposition of TiO_2 paste on FTO glass using Dr blading technique
- Annealing of deposited films
- Sensitizing the TiO_2 layers
- Preparation of counter electrode
- Injecting the electrolyte into the cells

Table 5: Equipment used for Production and Characterisation of the Cells:

S/N	EQUIPMENTS	Model	Manufacturer	USES
1	UV – Vis Spectrometer	1800 Series	Shimadzu, Japan	was used in measuring the absorbance of a particular layer
2	Solar simulator	Ketthley Series		was used to evaluate the performance of the cell
3	CVD	XD-1200NT	BioVac Inc.	Synthesis of CNTs
4	Magnetic Stirrer	Model 400	Gallenkamp, England	Stirring in the production of catalysts and CNTs

Preparation of FTO glass substrate

Plate 3: FTO glass preparation process

FTO glass with TiO_2 deposited on and annealing at 500 °C in air

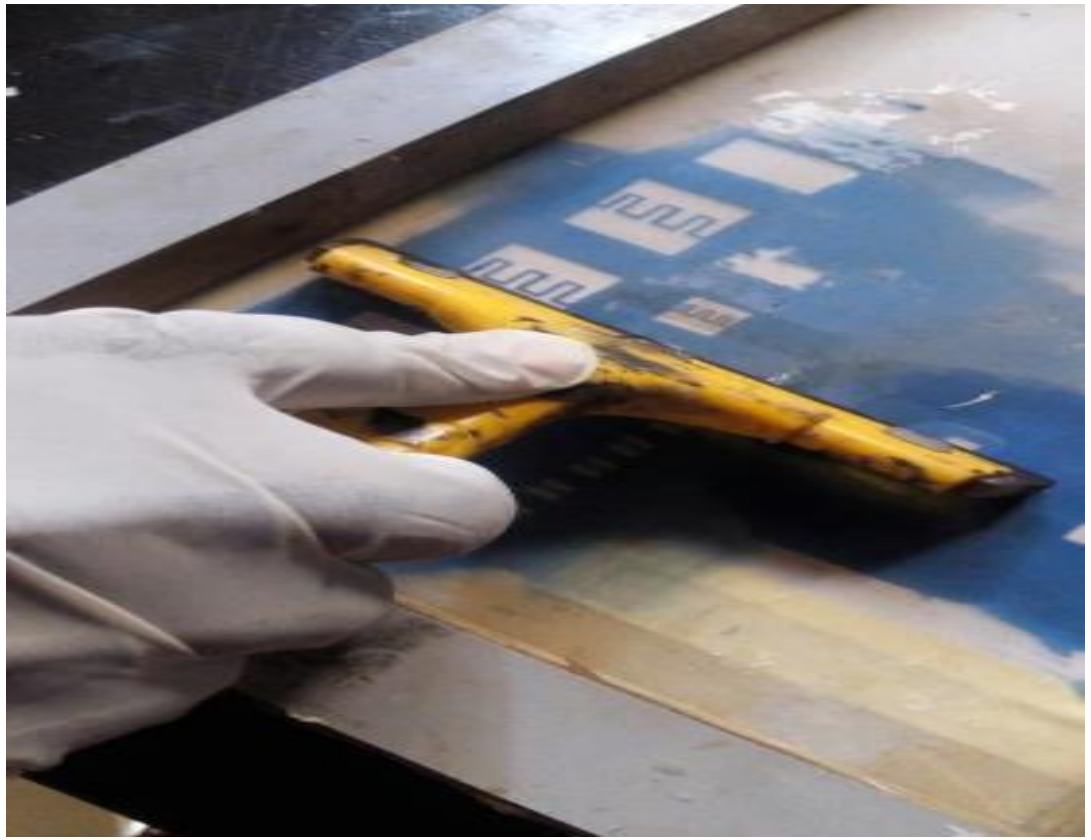

0.5 g of Pt-MWCNT + 10 ml of Texanol + 5 ml Acrylic resins mixed together to form a paste screen print on the glass substrate

Plate 4: (a) and (b): FTO glass with TiO_2 annealing at 500 °C and screen printing of paste of Pt-MWCNTs on FTO glass with TiO_2 compact layer, TiO_2 mesoporous layer and the dye

RESULTS AND DISCUSSION

UV-Vis optical absorbance analysis:

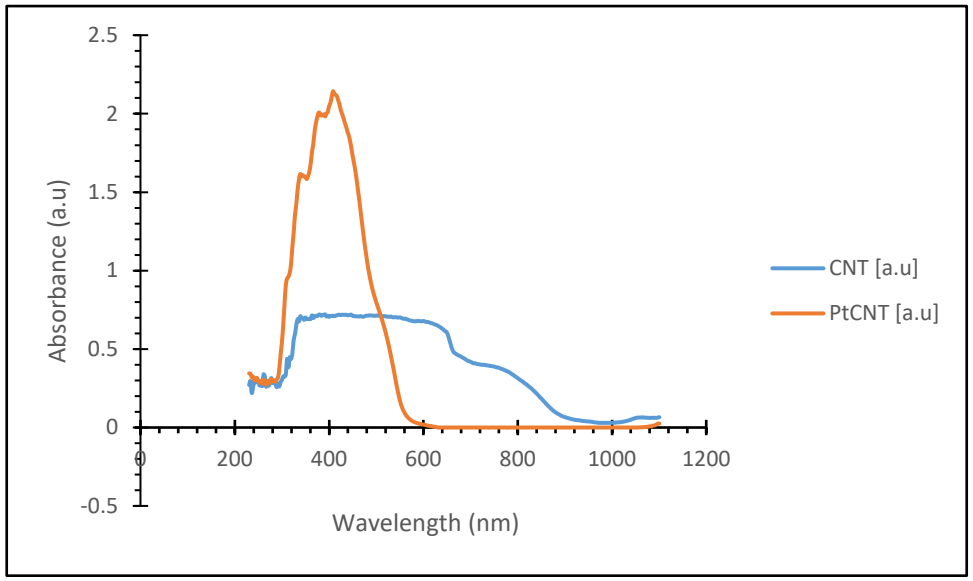

Figure 19: PEAK Absorbance of CNTs and Pt-MWCNTs

The optical band gap of cells were evaluated from the

absorption spectra using Tauc plot and using the equation

$\alpha h\nu = A\,(h\nu - E_g)^n$

Where:

A is constant, Eg is band gap, n is different allowed transition

Optical band gap of CNT 1.62

Optical band gap of Pt-MWCNT 2.52

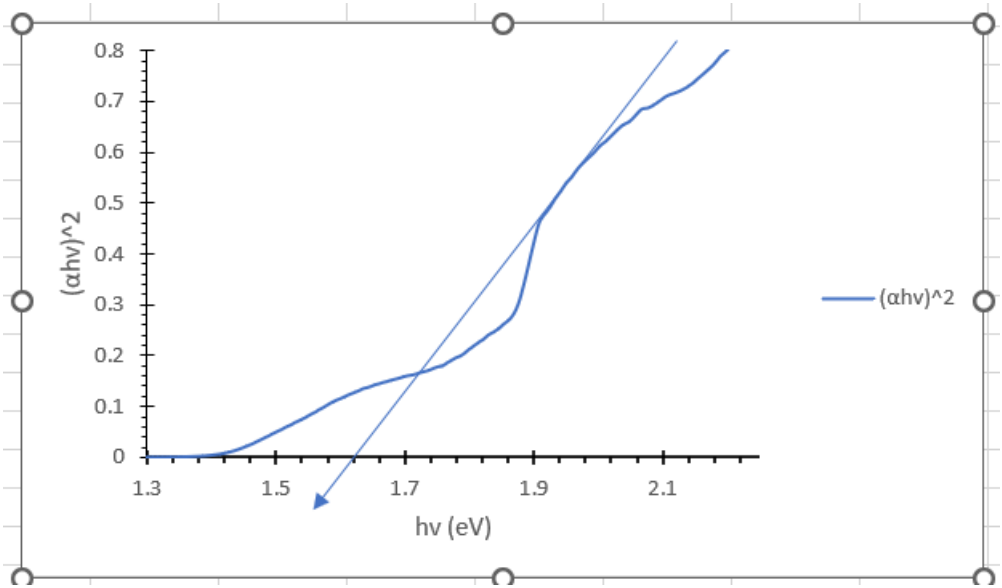

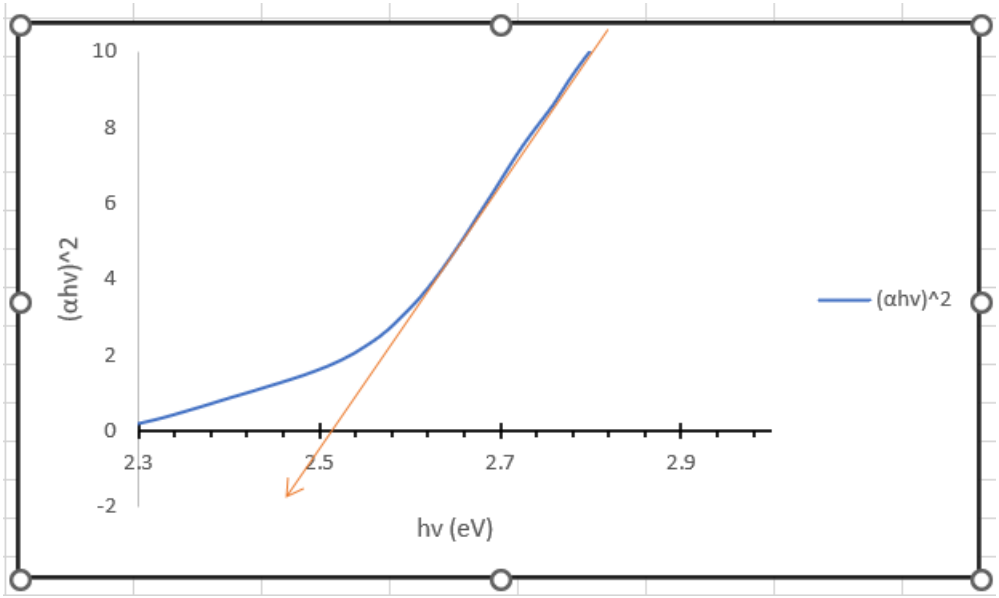

Figure 20: Band gap energy of MWCNTs and Pt-MWCNTs

Current-voltage analysis

The efficiency of the cells was calculated by the product of Voc, Jsc and *FF* divided by a Voc of 100mW/cm^2. It was under an illumination of AM 1.5 (P_{in}).

The formula that was used for the fill factor (FF) and efficiency are:

FF (fill factor) = $\frac{P_{max}}{(V_{oc} \times I_{sc})}$

$\eta = \left(\frac{P_{max}}{P_{in}}\right)$ x 100

MWCNTs

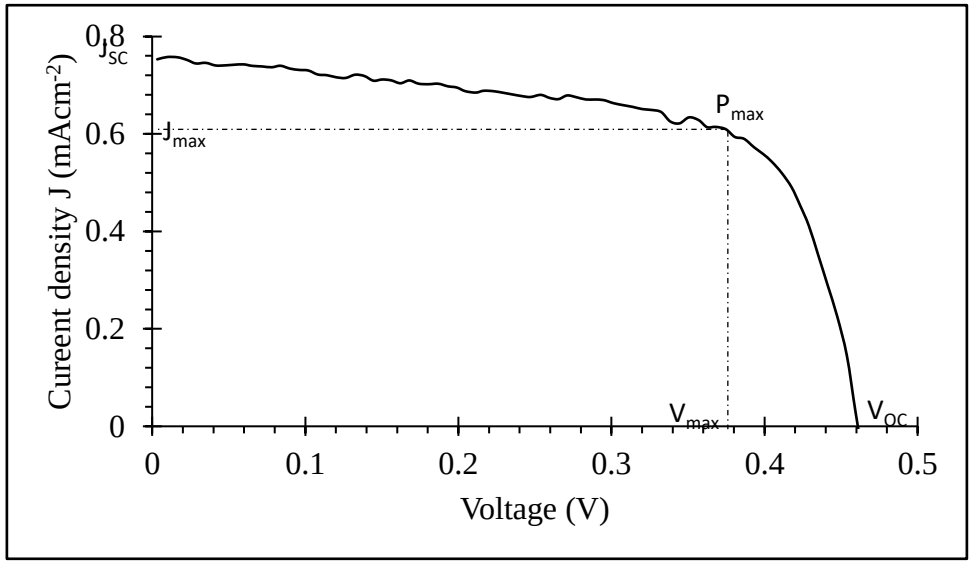

Figure 21: I-V Curve of MWCNTs

DSSC Efficiency FOR MWCNTS WAS CALCULATED AS:

$J_{max} = 0.61\ mAcm^{-2}$

$V_{max} = 0.38V$

$J_{sc} = 0.75\ mAcm^{-2}$

$V_{oc} = 0.46V$

$$\text{Fill factor (FF)} = \frac{P_{max}}{V_{oc}J_{sc}} = \frac{V_{max}J_{max}}{V_{oc}J_{sc}}$$

$$FF = \frac{0.38\times0.61}{0.46\times0.75} = \frac{0.23}{0.35} = 0.66$$

$$\eta = \frac{FF.V_{oc}.J_{sc}}{P_{in}} = \frac{0.66\times0.46\times0.75}{100} \times 100 = 0.28\%$$

Pt-MWCNT

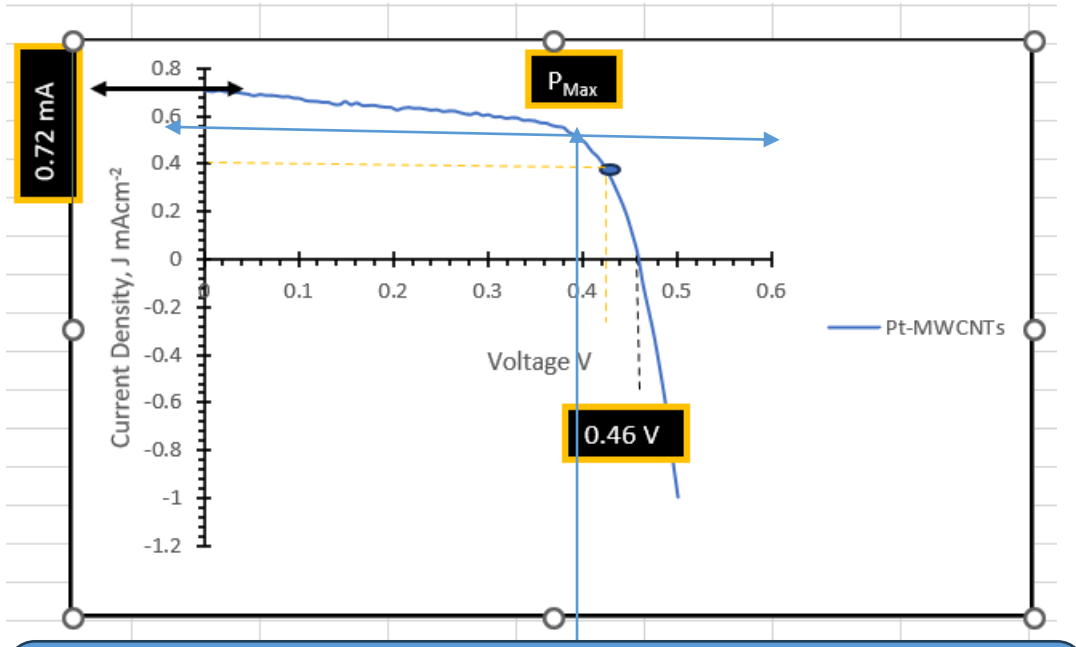

Figure 22: I-V Curve of Pt-MWCNTs

DSSC Efficiency FOR Pt-MWCNTS WAS CALCULATED AS:

$J_{max} = 0.40\ mAcm^{-2}$

$V_{max} = 0.41V$

$J_{sc} = 0.72\ mAcm^{-2}$

$V_{oc} = 0.46V$

$$\text{Fill factor (FF)} = \frac{P_{max}}{V_{oc}J_{sc}} = \frac{V_{max}J_{max}}{V_{oc}J_{sc}}$$

$$FF = \frac{0.42\times0.40}{0.46\times0.72} = \frac{1.7}{0.33}. = 5.15$$

$$\eta = \frac{FF.V_{oc}.J_{sc}}{P_{in}} = \frac{5.15\times0.46\times0.72}{100} \times 100 = 1.71\ \%$$

ECOLCARB

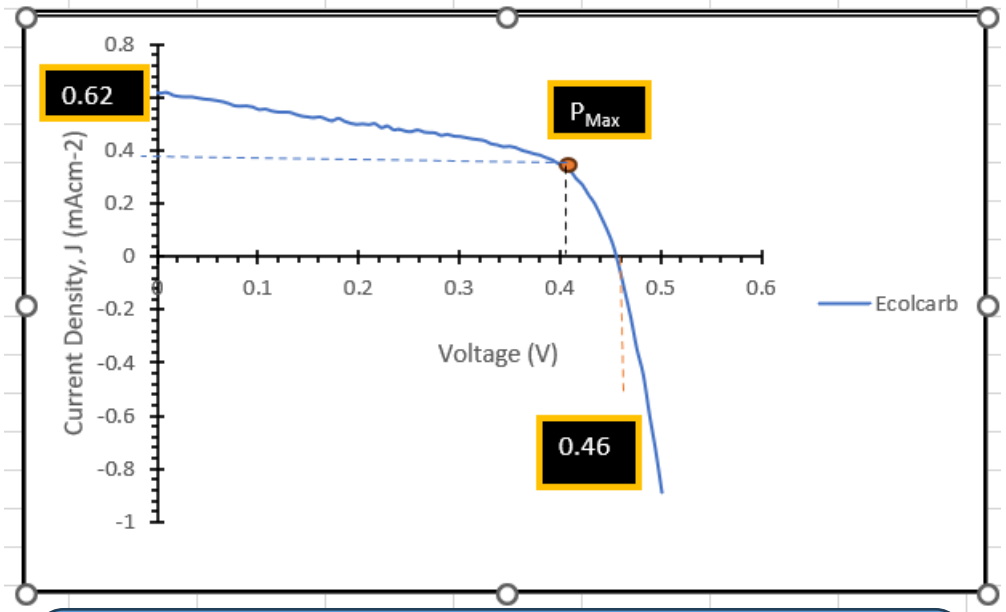

Figure 23: I-V Curve of Elcocarb

DSSC Efficiency FOR ECOLCARB WAS CALCULATED AS:

$J_{max} = 0.39\ mAcm^{-2}$

$V_{max} = 0.41V$

$J_{sc} = 0.62\ mAcm^{-2}$

$V_{oc} = 0.46V$

$$\text{Fill factor (FF)} = \frac{P_{max}}{V_{oc}J_{sc}} = \frac{V_{max}J_{max}}{V_{oc}J_{sc}}$$

$$FF = \frac{0.41\times0.39}{0.46\times0.62} = \frac{0.16}{0.35} = 0.56$$

$$\eta = \frac{FF.V_{oc}.J_{sc}}{P_{in}} = \frac{0.56\times0.46\times0.62}{100}\times 100 = 0.16$$

Current-Voltage Analysis

Table 6 : I-V Characterisation Parameters of DSSC with MWCNTs, Pt-MWCNT and Elcocarb

Counter Electrode	V_{OC}	J_{SC}	FF	η (%)	*Band gap (eV)*
MWCNTs	0.46	0.62	0.66	0.28	1.562
Pt-MWCNT	0.46	0.72	5.15	1.71	2.52
Ecolcarb	0.46	0.62	0.16	0.16	

CONCLUSION

i. Optimisation and preparation of Fe-Co/$CaCO_3$ catalyst was achieved by method of wet impregnation with the best catalyst yield of 95.71 %.

ii. The SEM/HRTEM/XRD analysis confirmed that multiwalled CNTs were produced with sizes ranging from 1.8 nm to 12.1 nm.

iii. UV spectroscopy shows that the quantity of Pt deposited on the surface of CNTs depend on the time of deposition when all other factors are kept constant.

iv. DSSCs with Pt-MWCNTs as counter electrode give a better efficiency than MWCNTs and Elcocarb.

RECOMMENDATIONS

i. Further work on how to increase the efficiency of the cell need to be looking into.

ii. The stability of DSSCs still a challenge; therefore, the issue need to be address properly for the purpose of its commercialisation

iii. To encourage researchers working on renewable energy especially solar cell, a functional solar simulator is required, therefore government should provide our research institutions with this machine.

REFERENCE

Abdulkareem, A. S., Suleiman, B., Abdulazeez, A. T., Kariim, I., Abubakre, O. K. and Afolabi, A. S., (2016). Synthesis and Characterisation of Carbon nanotubes on Fe/Al_2O_3 Composite Catalyst by Chemical Vapour deposition Method. *Proceedings of the World Congress on Engineering and Computer Science, San Francisco, USA*, 11. Retrieved February 2017. ISBN: 978-988-14048-2-4

Afolabi, A. S., Abdulkareem, A. S., Mhlanga, S. D., & Iyuke, S. E. (2011). "Synthesis and purification of bimetallic catalysed carbon nanotubes in a horizontal CVD reactor". *Journal of Experimental Nanoscience, 6*(3), 248-262

Afolabi, A. S. (2009). Development of carbon nanotubes platinum electro catalytic electrodes for proton exchange membrane fuel cell. Unpublished PhD thesis, *University of the Witwatersrand, Faculty of Engineering and the Built Environment. Johannesburg, South Africa*, 65-80.

Al-Fatesh, A. S. A. and Fakeeha, A. H., (2012). Effects of calcination and activation temperature on dry reforming catalysts. *Journal of Saudi Chemical Society*, 16, 55-61

Aliyu, A., Abdulkareem, A. S., Kovo, A. S., Abubakre, O. K., Tijani, J. O., Kariim, I. (2017). Synthesize multi-walled carbon nanotubes via catalytic chemical vapour deposition method on Fe-Ni bimetallic catalyst supported on kaolin. *Carbon Letters* , 21, 33-50.

REFERENCE Continues

Amjad, Z., (2014) *Mineral scales in biological and industrial systems*. CRC Press Taylor and Francis group London New Yolk.

Ball, J. M., Lee, M. M., Hey, A., Snaith, H. J., (2013). Low-temperature processed mesosuper structured to thin-film perovskite solar cells. *Energy Environmental Science*. 6, 1739–1743.

Chiwaye, N. (2012), "In Situ X-Ray Diffraction Analysis of Fischer Tropsch Synthesis". *Unpublished* MSc. Thesis, University of the Witwatersrand, Johannesburg.

Cruz-Gutiérrez, C.A., Félix-Navarro, R.M., Calva-Yañez, J.C. *et al.* (2021). Carbon nanotube-carbon black hybrid counter electrodes for dye-sensitized solar cells and the effect on charge transfer kinetics. *J Solid State Electrochem* **25**, 1479–1489. https://doi.org/10.1007/s10008-021-04932-y

Downs, R. T. (1993). Interactive software for calculating and displaying X -ray or neutron powder diffractometer patterns of crystalline materials. *American Mineralogist*, 78, 1104-1107.

Ibrahim, S., Kasim Uthman Isah, Abdulkareem, A. S., Umaru Ahmadu, Jimoh Oladejo Tijani, & Roos, W. (2020). Synthesis and characterization of platinum multi-walled carbon nanotubes nanocomposite film electrode. *Journal of Materials Science: Materials in Electronics*. https://doi.org/10.1007/s10854-020-03550-0

REFERENCE Continues

Amjad, Z., (2014) *Mineral scales in biological and industrial systems*. CRC Press Taylor and Francis group London New Yolk.

Shao, W., Wu, W. (2022) High-Efficiency (Over 10%) Parallel Tandem Dye-Sensitized Solar Cells Based on Tri-Carbon Electrodes. *Trans. Tianjin Univ.* **28**, 414–422. https://doi.org/10.1007/s12209-022-00318-x

TORLAK, Y., YENEL, E., & Metin, A. K. (2021). Fabrication and electrochemical properties of po lypyrol/multi-walled carbon nanotube composites for solar cell applications. *JOURNAL OF MATERIALS AND ELECTRONIC DEVICES*, *4*(1), 9-14.

Trunschke, A. (2013). Surface Area and Pore Size Determination. *Modern Methods in Modern Methods in Heterogeneous Catalysis Research*, 1-18

THANK YOU FOR LISTINING